TABLE 7. FACTORS ASSOCIATING WITH NODULE HYPOECHOGENICITY, LOGISTIC REGRESSION ANALYSIS

Factor	*Comparison*	*Odds ratio*	*95% CI*	p-*Value*[a]
Sex	Male vs. female	0.26	0.08–0.72	0.012
Halo	Absent vs. present	26.37	4.24–522.49	0.003
Calcifications	Absent vs. present	25.42	3.64–525.31	0.005

[a]Based on the likelihood ratio test.
CI, confidence interval.

be interesting to analyze a correlation between US, clinicopathological, and molecular features, first of all RET/PTC3 and RET/PTC1 rearrangements, in a specially designed study.

The irregular nodule margins on US are common in thyroid malignancy (1,3,9–11,13–16,30,31). An analysis done by Papini *et al.* demonstrated that independent risk factors of cancer at US of nonpalpable thyroid nodules were irregular or blurred nodule margins, intranodular vascular pattern, and microcalcifications (13). Another study has identified nodule margins and shape, internal echo level, but not "strong echoes" (calcifications) as important characteristics in differentiating papillary thyroid carcinoma from benign neoplasm (10). Our findings are in agreement with these studies only for the tumors exceeding 10 mm in diameter. The importance of irregular margins as criterion of malignancy was significantly weaker in smaller tumors. Technically, it is not surprising that irregular margins are found less frequently in very small thyroid nodules by US because of limited resolution of the latter.

The associations between cancer nodule size, type of margin, and latent period are also worth noting. The longer latent period was characteristic to the nodules with regular margins, which may reflect the difficulties of early diagnosis of slowly growing tumors. Radiation-induced thyroid carcinomas developing after the shorter period of latency are often in advanced stage, are aggressive at presentation, and display elevated risk of recurrence despite the small size (5,32–34). It is therefore necessary to take into account that the nodules detected after the longer latency may display less unusual suspicious signs on US, yet they may well be malignant.

Regarding tumor echogenicity, hypoechoic nodules are more likely to be malignant in contrast to those lacking such characteristics (10,11,15–17), especially if nodule size exceeds 15 mm (35). In our series hypoechogenicity was associated with female sex, and the absence of both halo and calcifications, while isoechogenicity with male sex (this observation is difficult to explain). Note also that nodule hypoechogenicity was more frequently observed in younger patients and after the shorter period of latency which together are supportive of the overall suspicious nature of this US feature.

From the practical point of view, the clinical decision to biopsy a small thyroid nodule in children or young patients is not simple and has individual and overall healthcare cost implications (36). If we used nodule diameter of 10 mm as cut-off for FNAB, we would have missed 25 (26.6%) cases of thyroid cancer in our young patients. Papini *et al.* obtained a very similar result in a prospective study of 402 nodules (13). If FNAB had been restricted to the nodules exceeding 10 mm in size, cytological evaluation would have been omitted in 38.7% of the actually diagnosed malignancies. They proposed a cut-off diameter of 8 mm for nonpalpable nodules to be subjected to cytological evaluation, while follow-up of the smaller lesions was recommended. The findings presented here support the results of prior studies that showed that nodule size greater or smaller than 10 mm was not an effective arbitrary criterion for FNAB (8,13,37,38) as well as that probability of malignancy in thyroid nodules measuring less than 1 cm is not lower than in larger lesions (39). From this point of view, our results also support the necessity of evaluation of small thyroid nodules in radiation-exposed patients recommended by the American Thyroid Association (9) and the American Association of Clinical Endocrinologists and Associazione Medici Endocrinologi (23).

In addition to the nodule size issues, if we biopsied only nodules with irregular margins, 20 (21.7%) cases would have been missed. If we biopsied only usual suspicious hypoechoic nodules, we would have missed 22 isoechoic tumors and 17 nodules with mixed echogenicity (41.9% cases combined). Further, as shown in our previous study, the relative proportion of cancer nodules among all thyroid nodules detected in young individuals affected by the Chernobyl fallouts decreases with time after exposure due to the increasing prevalence of nodular goiter, nonverified small solid nodules, and cysts (3). In some sense this may predispose to the intuitive expectation of a benign rather than cancerous nodule to be developing after the longer latency. In our opinion, physicians need to be aware of that the situation is more complex.

This study demonstrates that important US features considered usual for thyroid cancer are less frequent in smaller tumors and that thyroid cancers developing with a greater latency after radiation are less likely to have worrisome US features. We therefore propose that in young individuals with a history of internal radiation exposure FNAB should be recommended even for small thyroid nodules (i.e., whenever technically accessible) with any margin type and echogenicity.

Acknowledgment

This work was supported in part by Nagasaki University Global COE program.

Disclosure Statement

The authors declare that no competing financial interests exist.

References

1. Hegedus L 2004 Clinical practice. The thyroid nodule. N Engl J Med **351**:1764–1771.
2. Reiners C, Wegscheider K, Schicha H, Theissen P, Vaupel R, Wrbitzky R, Schumm-Draeger PM 2004 Prevalence of thyroid disorders in the working population of Germany: ultrasonography screening in 96,278 unselected employees. Thyroid **14**:926–932.
3. Drozd V, Polyanskaya O, Ostapenko V, Demidchik Y, Biko I, Reiners C 2002 Systematic ultrasound screening as a

significant tool for early detection of thyroid carcinoma in Belarus. J Pediatr Endocrinol Metab **15**:979–984.
4. Imaizumi M, Usa T, Tominaga T, Akahoshi M, Ashizawa K, Ichimaru S, Nakashima E, Ishii R, Ejima E, Hida A, Soda M, Maeda R, Nagataki S, Eguchi K 2005 Long-term prognosis of thyroid nodule cases compared with nodule-free controls in atomic bomb survivors. J Clin Endocrinol Metab **90**:5009–5014.
5. Bucci A, Shore-Freedman E, Gierlowski T, Mihailescu D, Ron E, Schneider AB 2001 Behavior of small thyroid cancers found by screening radiation-exposed individuals. J Clin Endocrinol Metab **86**:3711–3716.
6. Shevchuk VE, Gurachevsky GV (eds) 2006 20 Years after the Chernobyl Catastrophe. Publishing House Belarus, Minsk, Belarus, p 250.
7. Baskin HJ 2004 Thyroid ultrasound—just do it. Thyroid **14**:91–92.
8. Frates MC, Benson CB, Doubilet PM, Kunreuther E, Contreras M, Cibas ES, Orcutt J, Moore FD Jr., Larsen PR, Marqusee E, Alexander EK 2006 Prevalence and distribution of carcinoma in patients with solitary and multiple thyroid nodules on sonography. J Clin Endocrinol Metab **91**:3411–3417.
9. Cooper DS, Doherty GM, Haugen BR, Kloos RT, Lee SL, Mandel SJ, Mazzaferri EL, McIver B, Sherman SI, Tuttle RM 2006 Management guidelines for patients with thyroid nodules and differentiated thyroid cancer. Thyroid **16**:109–142.
10. Shimura H, Haraguchi K, Hiejima Y, Fukunari N, Fujimoto Y, Katagiri M, Koyanagi N, Kurita T, Miyakawa M, Miyamoto Y, Suzuki N, Suzuki S, Kanbe M, Kato Y, Murakami T, Tohno E, Tsunoda-Shimizu H, Yamada K, Ueno E, Kobayashi K, Kobayashi T, Yokozawa T, Kitaoka M 2005 Distinct diagnostic criteria for ultrasonographic examination of papillary thyroid carcinoma: a multicenter study. Thyroid **15**:251–258.
11. Tae HJ, Lim DJ, Baek KH, Park WC, Lee YS, Choi JE, Lee JM, Kang MI, Cha BY, Son HY, Lee KW, Kang SK 2007 Diagnostic value of ultrasonography to distinguish between benign and malignant lesions in the management of thyroid nodules. Thyroid **17**:461–466.
12. Wienke JR, Chong WK, Fielding JR, Zou KH, Mittelstaedt CA 2003 Sonographic features of benign thyroid nodules: interobserver reliability and overlap with malignancy. J Ultrasound Med **22**:1027–1031.
13. Papini E, Guglielmi R, Bianchini A, Crescenzi A, Taccogna S, Nardi F, Panunzi C, Rinaldi R, Toscano V, Pacella CM 2002 Risk of malignancy in nonpalpable thyroid nodules: predictive value of ultrasound and color-Doppler features. J Clin Endocrinol Metab **87**:1941–1946.
14. Koike E, Noguchi S, Yamashita H, Murakami T, Ohshima A, Kawamoto H, Yamashita H 2001 Ultrasonographic characteristics of thyroid nodules: prediction of malignancy. Arch Surg **136**:334–337.
15. Rago T, Vitti P, Chiovato L, Mazzeo S, De Liperi A, Miccoli P, Viacava P, Bogazzi F, Martino E, Pinchera A 1998 Role of conventional ultrasonography and color flow-doppler sonography in predicting malignancy in 'cold' thyroid nodules. Eur J Endocrinol **138**:41–46.
16. Chan BK, Desser TS, McDougall IR, Weigel RJ, Jeffrey RB Jr. 2003 Common and uncommon sonographic features of papillary thyroid carcinoma. J Ultrasound Med **22**:1083–1090.
17. Peccin S, de Castsro JA, Furlanetto TW, Furtado AP, Brasil BA, Czepielewski MA 2002 Ultrasonography: is it useful in the diagnosis of cancer in thyroid nodules? J Endocrinol Invest **25**:39–43.
18. Pellegriti G, Scollo C, Lumera G, Regalbuto C, Vigneri R, Belfiore A 2004 Clinical behavior and outcome of papillary thyroid cancers smaller than 1.5 cm in diameter: study of 299 cases. J Clin Endocrinol Metab **89**:3713–3720.
19. Brunn J, Block U, Ruf G, Bos I, Kunze WP, Scriba PC 1981 Volumetrie der Schilddrüsenlappen mittels Real-Time-Sonographie. Dtsch Med Wochenschr **106**:1338–1340.
20. Sobin LH, Wittekind CH (eds) 2002 International Union Against Cancer. TNM Classification of Malignant Tumors, sixth edition. John Wiley & Sons, Inc., New York, p 239.
21. SAS Institute 1999 SAS/STAT User's Guide Version 8. SAS Institute, Cary, NC.
22. Frates MC, Benson CB, Charboneau JW, Cibas ES, Clark OH, Coleman BG, Cronan JJ, Doubilet PM, Evans DB, Goellner JR, Hay ID, Hertzberg BS, Intenzo CM, Jeffrey RB, Langer JE, Larsen PR, Mandel SJ, Middleton WD, Reading CC, Sherman SI, Tessler FN 2005 Management of thyroid nodules detected at US: Society of Radiologists in Ultrasound consensus conference statement. Radiology **237**:794–800.
23. AACE/AME Task Force on Thyroid Nodules 2006 American Association of Clinical Endocrinologists and Associazione Medici Endocrinologi medical guidelines for clinical practice for the diagnosis and management of thyroid nodules. Endocr Pract **12**:63–102.
24. Hay ID, Grant CS, van Heerden JA, Goellner JR, Ebersold JR, Bergstralh EJ 1992 Papillary thyroid microcarcinoma: a study of 535 cases observed in a 50-year period. Surgery **112**:1139–1146; discussion 1146–1147.
25. Mazzaferri EL, Massoll N 2002 Management of papillary and follicular (differentiated) thyroid cancer: new paradigms using recombinant human thyrotropin. Endocr Relat Cancer **9**:227–247.
26. Cappelli C, Castellano M, Braga M, Gandossi E, Pirola I, De Martino E, Agosti B, Rosei EA 2007 Aggressiveness and outcome of papillary thyroid carcinoma (PTC) versus microcarcinoma (PMC): a mono-institutional experience. J Surg Oncol **95**:555–560.
27. Alexander EK, Heering JP, Benson CB, Frates MC, Doubilet PM, Cibas ES, Marqusee E 2002 Assessment of nondiagnostic ultrasound-guided fine needle aspirations of thyroid nodules. J Clin Endocrinol Metab **87**:4924–4927.
28. Nikiforov YE, Rowland JM, Bove KE, Monforte-Munoz H, Fagin JA 1997 Distinct pattern of ret oncogene rearrangements in morphological variants of radiation-induced and sporadic thyroid papillary carcinomas in children. Cancer Res **57**:1690–1694.
29. Rabes HM, Demidchik EP, Sidorow JD, Lengfelder E, Beimfohr C, Hoelzel D, Klugbauer S 2000 Pattern of radiation-induced RET and NTRK1 rearrangements in 191 post-Chernobyl papillary thyroid carcinomas: biological, phenotypic, and clinical implications. Clin Cancer Res **6**: 1093–1103.
30. Takashima S, Fukuda H, Nomura N, Kishimoto H, Kim T, Kobayashi T 1995 Thyroid nodules: re-evaluation with ultrasound. J Clin Ultrasound **23**:179–184.
31. Kim EK, Park CS, Chung WY, Oh KK, Kim DI, Lee JT, Yoo HS 2002 New sonographic criteria for recommending fine-needle aspiration biopsy of nonpalpable solid nodules of the thyroid. AJR Am J Roentgenol **178**:687–691.
32. Williams ED, Becker D, Dimidchik EP, Nagataki S, Pinchera A, Tronko ND 1996 Effects on the thyroid in populations exposed to radiation as a result of the Chernobyl accident.

In: Demir M (ed) One Decade after Chernobyl: Summing up the Consequences of the Accident. International Atomic Energy Authority, Vienna, pp 207–230.
33. Farahati J, Demidchik EP, Biko J, Reiners C 2000 Inverse association between age at the time of radiation exposure and extent of disease in cases of radiation-induced childhood thyroid carcinoma in Belarus. Cancer **88**:1470–1476.
34. Demidchik YE, Demidchik EP, Reiners C, Biko J, Mine M, Saenko VA, Yamashita S 2006 Comprehensive clinical assessment of 740 cases of surgically treated thyroid cancer in children of Belarus. Ann Surg **243**:525–532.
35. Lyshchik A, Drozd V, Demidchik Y, Reiners C 2005 Diagnosis of thyroid cancer in children: value of gray-scale and power doppler US. Radiology **235**:604–613.
36. Rosen JE, Stone MD 2006 Contemporary diagnostic approach to the thyroid nodule. J Surg Oncol **94**:649–661.
37. Davies TF 2006 Is consensus a good thing in the management of thyroid nodules? Thyroid **16**:205.
38. Burman KD 2006 Micropapillary thyroid cancer: should we aspirate all nodules regardless of size? J Clin Endocrinol Metab **91**:2043–2046.
39. Berker D, Aydin Y, Ustun I, Gul K, Tutuncu Y, Isik S, Delibasi T, Guler S 2008 The value of fine-needle aspiration biopsy in subcentimeter thyroid nodules. Thyroid **18**:603–608.

Address correspondence to:
Vladimir A. Saenko, Ph.D.
Department of International Health and Radiation Research
Nagasaki University Graduate School of Biomedical Sciences
1-12-4 Sakamoto
Nagasaki 852-8523
Japan

E-mail: saenko@net.nagasaki-u.ac.jp

THYROID
Volume 19, Number 8, 2009

DOI: 10.1089/thy.2009.0059

Lack of GNAQ Hotspot Mutation in Papillary Thyroid Carcinomas

Michiko Matsuse,[1] Norisato Mitsutake,[1] Eijun Nishihara,[2] Tatiana Rogounovitch,[1] Vladimir Saenko,[3] Pavel Rumyantsev,[4] Eugeny Lushnikov,[5] Keiji Suzuki,[1] Akira Miyauchi,[2] and Shunichi Yamashita[1,3]

Dear Editor:

Papillary thyroid carcinoma (PTC) is the most common malignant tumor in endocrine organs. PTCs have characteristic gene mutations leading to the activation of mitogen-activated protein kinase (MAPK) signaling pathway. Those include *RET/PTC* rearrangements and point mutations in *BRAF* and *RAS* family genes. They are found in approximately 60–70% of all PTCs and rarely overlap in the same tumor (1–3). The absence of coexistence of those mutations provides strong genetic evidence for the requirement of constitutively active MAPK signaling for transformation to PTC. However, the remaining 30–40% of PTC cases do not have mutations in those genes, suggesting that other factors may contribute to constitutive activation of the MAPK pathway.

Similar to PTCs, most melanomas harbor oncogenic mutations in the MAPK signaling components—in particular, *BRAF* and *RAS*; however, a subset of melanomas including uveal melanoma does not have mutations in those genes. Very recently, frequent somatic mutations in the *GNAQ* gene have been identified in uveal melanomas and blue naevi (4,5). *GNAQ* encodes members of the q class of G-protein α-subunits involved in mediating signals from G-protein-coupled receptors. Several patterns of mutations have been found (at nucleotides 625–627, wild-type CAA to CTA, TTA, CCA, CAT, CGA or TAT), but all the mutations exclusively occur in codon 209 in the RAS-like domain, which corresponds to codon 61 of RAS, and result in constitutive activation of the MAPK pathway in melanocytes (4). There is no equivalent of RAS codon 12 in GNAQ. Signaling from GNAQ to MAPK seems to be transmitted through diacylglycerol/protein kinase C (4,6). The *GNAQ* mutations have not been described in other human neoplasms so far. However, $GNAQ^{Q209L}$ mutation, which is indeed dominant type of mutation found in blue naevi and uveal melanomas, was already shown to have an ability to transform NIH3T3 cells (7).

Although it remains to be tested whether GNAQ can activate the MAPK pathway in thyroid cells, GNAQ seems to be a good candidate as a target of oncogenic mutation in PTCs. In this study, therefore, the possibility that *GNAQ* mutation plays a role in PTC pathogenesis was explored.

First of all, we investigated Russian PTC samples that were obtained at the time of surgery in the Medical Radiological Research Center of Russian Academy of Medical Sciences (Obninsk, Russia); none of the patients had a history of radiation exposure. An informed consent was obtained from each individual according to ethical guidelines for the use of human materials for scientific purposes effective in Medical Radiological Research Center of Russian Academy of Medical Sciences. Protocol for the present study was approved by the Committee for Ethical Issues of Human Genome Analysis in Nagasaki University. All samples were collected at the time of primary surgery and did not include recurrence. Forty-two PTC frozen samples from 36 patients (36 primary tumors and 6 metastatic lymph nodes, no multiple cancer) without *RET/PTC1*, *RET/PTC3*, $BRAF^{V600E}$, or hotspot mutations (codons 12, 13, and 61) in three *RAS* genes (*HRAS*, *KRAS*, and *NRAS*) were subjected to DNA extraction (conventional proteinase K/phenol protocol). The same set of samples was used for the analysis of *RAP1* mutation, and the clinicopathological characteristics of the patients were described previously (8). Amplification of the *GNAQ* gene was then performed by genomic PCR using AmpliTaq Gold (Applied Biosystems, Foster City, CA). The sequences of used primers are same as previously described (4). PCR products were then treated with ExoSAP-IT (USB, Cleveland, OH), and sequence analysis was performed with a Big Dye Terminator sequencing kit v3.1 (Applied Biosystems) and an ABI3100 automated sequencer (Applied Biosystems). As a result, no mutation was found around hotspot codon 209 in the *GNAQ* gene.

We next used 46 Japanese PTC samples collected at Kuma Hospital (Kobe, Japan). All samples were primary tumors from different individuals. An appropriate informed consent was obtained from each individual, and the protocol was

[1]Department of Molecular Medicine, Atomic Bomb Disease Institute, Nagasaki University Graduate School of Biomedical Sciences, Nagasaki, Japan.
[2]Kuma Hospital, Kobe, Japan.
[3]Department of International Health and Radiation Research, Atomic Bomb Disease Institute, Nagasaki University Graduate School of Biomedical Sciences, Nagasaki, Japan.
Departments of [4]Radiosurgery and [5]Pathology, Medical Radiological Research Center, Obninsk, Russia.

approved by the ethics committees of Nagasaki University and Kuma Hospital. We performed the sequence analysis using all 46 samples regardless of existence of other oncogenes. Of note, among 46 samples, there were 36 *BRAF*^{V600E}, 3 *RET/PTC1*, and no *RET/PTC3* nor *RAS* mutation (without overlap). Again, no mutations were identified in the *GNAQ* gene.

Based on these findings, we conclude that the *GNAQ* hotspot mutation is unlikely to play an important role in the molecular pathogenesis of PTCs.

Acknowledgments

This work was supported in part by Grant-in-Aid for Scientific Research (#19256003, #19390253, #19790651, and #20790662) and Global COE Program from the Ministry of Education, Culture, Sports, Science, and Technology of Japan.

References

1. Frattini M, Ferrario C, Bressan P, Balestra D, De Cecco L, Mondellini P, Bongarzone I, Collini P, Gariboldi M, Pilotti S, Pierotti MA, Greco A 2004 Alternative mutations of BRAF, RET and NTRK1 are associated with similar but distinct gene expression patterns in papillary thyroid cancer. Oncogene **23**:7436–7440.
2. Kimura ET, Nikiforova MN, Zhu Z, Knauf JA, Nikiforov YE, Fagin JA 2003 High prevalence of BRAF mutations in thyroid cancer: genetic evidence for constitutive activation of the RET/PTC-RAS-BRAF signaling pathway in papillary thyroid carcinoma. Cancer Res **63**:1454–1457.
3. Soares P, Trovisco V, Rocha AS, Lima J, Castro P, Preto A, Maximo V, Botelho T, Seruca R, Sobrinho-Simoes M 2003 BRAF mutations and RET/PTC rearrangements are alternative events in the etiopathogenesis of PTC. Oncogene **22**:4578–4580.
4. Van Raamsdonk CD, Bezrookove V, Green G, Bauer J, Gaugler L, O'Brien JM, Simpson EM, Barsh GS, Bastian BC 2009 Frequent somatic mutations of GNAQ in uveal melanoma and blue naevi. Nature **457**:599–602.
5. Onken MD, Worley LA, Long MD, Duan S, Council ML, Bowcock AM, Harbour JW 2008 Oncogenic mutations in GNAQ occur early in uveal melanoma. Invest Ophthalmol Vis Sci **49**:5230–5234.
6. Hubbard KB, Hepler JR 2006 Cell signalling diversity of the Gqalpha family of heterotrimeric G proteins. Cell Signal **18**:135–150.
7. Kalinec G, Nazarali AJ, Hermouet S, Xu N, Gutkind JS 1992 Mutated alpha subunit of the Gq protein induces malignant transformation in NIH 3T3 cells. Mol Cell Biol **12**:4687–4693.
8. Matsuse M, Mitsutake N, Rogounovitch T, Saenko V, Nakazawa Y, Rumyantsev P, Lushnikov E, Suzuki K, Yamashita S 2009 Mutation analysis of RAP1 gene in papillary thyroid carcinomas. Endocr J **56**:161–164.

Address correspondence to:
Norisato Mitsutake, M.D., Ph.D.
Department of Molecular Medicine
Atomic Bomb Disease Institute
Nagasaki University Graduate School of Biomedical Sciences
1-12-4 Sakamoto
Nagasaki 852-8523
Japan

E-mail: mitsu@nagasaki-u.ac.jp

Mutation Research 671 (2009) 33–39

Contents lists available at ScienceDirect

Mutation Research/Fundamental and Molecular Mechanisms of Mutagenesis

journal homepage: www.elsevier.com/locate/molmut
Community address: www.elsevier.com/locate/mutres

Long-term persistence of X-ray-induced genomic instability in quiescent normal human diploid cells

Keiji Suzuki[a,*], Genro Kashino[b], Seiji Kodama[c], Masami Watanabe[b]

[a] Course of Life Sciences and Radiation Research, Graduate School of Biomedical Sciences, Nagasaki University, 1-12-4 Sakamoto, Nagasaki 852-8523, Japan
[b] Kyoto University Research Reactor Institute, Kumatori-cho Sennan-gun, Osaka 590-0494, Japan
[c] Research Institute for Advanced Science and Technology, Osaka Prefecture University, 1-2 Gakuen-machi, Sakai 599-8570, Japan

ARTICLE INFO

Article history:
Received 26 May 2009
Received in revised form 16 July 2009
Accepted 18 August 2009
Available online 25 August 2009

Keywords:
Ionizing radiation
Instability
Chromosome
DNA damage
In vitro

ABSTRACT

Ionizing radiation can induce genomic instability in the progeny of irradiated cells, as was demonstrated in various experimental systems. Most *in vitro* studies have utilized replicating cells, but it is not clear whether radiation-induced genomic instability persists in quiescent cells. Here we show the induction of X-ray-induced genomic instability in normal human diploid cells irradiated and maintained in a quiescent state for up to 24 months while cells were subcultured approximately once every 2–3 months. Every 12 months, a fraction of the irradiated cell population was stimulated to divide by culturing at a low density, and we found that these cells showed increased frequencies of phosphorylated ATM foci, decreased colony-forming ability, and increased frequency of chromosomal aberrations. No significant increases in ROS levels were detected in long-term cultured cells. These results suggest that there are ROS-independent mechanism(s) induced by radiation, which can generate persistent delayed effects in quiescent cells, and could ultimately contribute to carcinogenesis.

1. Introduction

Accumulating evidence suggests that ionizing radiation can cause various delayed effects in cells that have not directly absorb radiation energy [1–5]. These effects, observed in non-irradiated cells, are now collectively described as non-targeted effects, which include radiation-induced genomic instability. Genomic instability is manifested in the progeny of surviving cells and is measured as the expression of various delayed effects such as delayed reproductive death or lethal mutation, delayed chromosomal instability, and delayed mutagenesis [6–9]. Since radiation-induced genomic instability leads to the accumulation of gene mutations and chromosomal rearrangements, it is thought to play a pivotal role in radiation-induced carcinogenesis [10–13].

Recent advances in stem cell biology suggest the possible involvement of tissue stem cells in the development of cancer [14–17]. Stem cells are able to proliferate both asymmetrically and symmetrically, and until they are stimulated to divide, some stem populations undergo quiescence in contact with a stem cell niche [18–22]. Such quiescence in niche has been hypothesized to account for why cancer stem cells are refractory to chemotherapy and radiotherapy [23,24]. In contrast to the proliferating tissue stem cells, whose surviving progenies manifest radiation-induced genomic instability during the successive cell divisions, survived quiescent stem cells remain residing in the radiation-exposed tissues until they face circumstances that trigger their proliferation and increase the risk of manifesting genomic instability. Since genetic changes leading to carcinoma are thought to accumulate in non-hematopoietic stem cells, and most of these cells remain in a quiescent state for the better part of their life span, it is highly relevant to examine the persistence of radiation-induced genomic instability in cells maintained in a quiescent state [17]. As reported recently, sustained excess relative risk of solid cancers demonstrated in atomic bomb survivors has suggested that radiation-exposed tissue stem cells residing in a niche may undergo proliferation after a long period of quiescence [25,26]. Thus, our present study was designed to determine whether or not irradiated cells that have remained in a quiescent state for long time are indeed capable of inducing delayed phenotypes after they are forced to divide. Current studies are also indispensable for the better understanding of the late effects of radiation, because non-cancerous late effects are also known to be stemmed from delayed dysfunction in stem cells of various adult tissues.

In the present study, normal human diploid cells were maintained in a confluent (quiescent) state for up to 24 months after irradiation. We found that those cells stimulated to divide after the confluence showed the delayed induction of DNA double strand breaks, as well as various delayed phenotypes, including delayed reproductive death and delayed chromosome instability, thereby indicating the persistence of radiation-induced genomic instability.

* Corresponding author.
E-mail address: kzsuzuki@nagasaki-u.ac.jp (K. Suzuki).

0027-5107/$ – see front matter © 2009 Elsevier B.V. All rights reserved.
doi:10.1016/j.mrfmmm.2009.08.010

Interestingly, no significant increase in ROS levels were detected in long-term cultured cells, which implicated ROS-independent mechanism(s) capable of contributing to the succession and perpetuation of the initial insults of the genome caused by ionizing radiation.

2. Materials and methods

2.1. Cell culture and irradiation

Normal human diploid fibroblast-like cells were cultured in MEM supplemented with 10% fetal bovine serum (TRACE Bioscience PTY Ltd., Australia) [27]. Exponentially growing cells were irradiated with an X-ray generator at 150 kVp and 5 mA with a 0.1-mm copper (SOFTEX M-150WE, Softex, Osaka). Cells remaining in a confluent state were irradiated at a dose rate with 0.44 Gy/min. After irradiation with 4 Gy, the cells were cultured in T75 flasks (75 cm^2) for up to 24 months, during which time the medium was changed every 2–3 days. At subculture, cell numbers were determined using a cell counter (Microcell Counter, Sysmex Co. Ltd., Tokyo). The population doubling numbers (PDNs) were calculated as follows: PDNs = $\ln(N_1/N_0)/\ln 2$, where N_1 and N_0 are the cell number at the end of each passage and the number of cells inoculated, respectively.

2.2. Analysis of delayed effects

The procedure used for the analysis of delayed effects is summarized in Fig. 1. Twelve and twenty-four months after irradiation, cells were collected by trypsinization and a portion of both the control and X-irradiated cells was kept on ice to examine ROS levels. Another portion of cells was grown in T75 flasks at a low density (1×10^6 cells/flaks), and these cells were cultured for an additional 3 and 7 days in order to examine any delayed DNA damage, delayed chromosomal instability, and to determine levels of ROS. Delayed induction of DNA double strand breaks was determined by examining phosphorylated ATM foci. After 3 and 7 days in culture, the cells were replated onto 22 mm × 22 mm cover slips for immunofluorescence study using monoclonal antibody against phosphorylated ATM protein. At the same time, another portion of the proliferating cells was plated onto 100-mm dishes at a clonal density (10^2 cells per 100 mm-dish) to determine delayed reproductive death and giant cell formation in the colonies. After 2 weeks of incubation, twenty formed colonies were randomly isolated from both populations, and the clonal cells were directly replated onto coverslips. Twenty-four hours after isolation, the cells were stained with monoclonal antibody against phosphorylated ATM protein.

2.3. Detection of delayed DNA damage

Delayed induction of DNA double strand breaks was determined by phosphorylated ATM foci as described previously [28]. Cells cultured on coverslips were fixed with 4% formaldehyde, permeabilized with 0.5% Triton X-100, and were washed extensively with phosphate-buffered saline (PBS). The primary antibodies, anti-phosphorylated ATM monoclonal antibody (Clone 10H11.E12, Rockland, Gilbertsville, PA) were diluted in 100 μl of TBS-DT (20 mM Tris–HCl, 137 mM NaCl, pH 7.6, containing 50 mg/ml skim milk and 0.1% Tween-20), and the antibody was applied on the coverslips. The samples were incubated for 2 h in a humidified CO_2 incubator at 37 °C. The primary antibody was washed with PBS, and Alexa488-labelled anti-mouse and anti-rabbit IgG antibodies (Molecular Probes, Inc., OR) were added. The coverslips were incubated for 1 h in a humidified CO_2 incubator at 37 °C, washed with PBS and counterstained with 0.1 mg/ml of DAPI. The samples were examined with a F300B fluorescence microscope (Leica, Tokyo). Digital images were captured and the images were analyzed by FW4000 software (Leica). The formation of phosphorylated ATM foci was determined in 10^3 cells for each group.

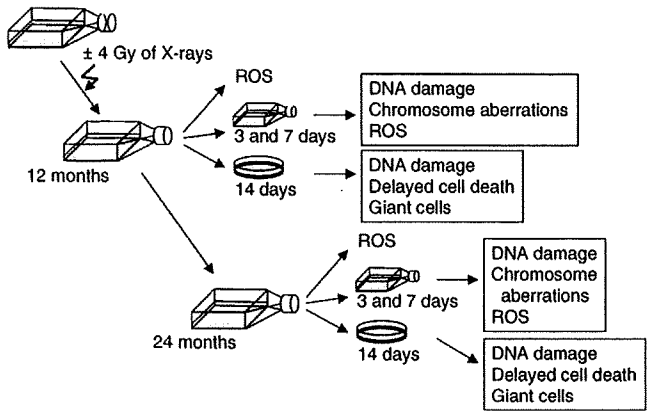

Fig. 1. Experimental procedure for the analysis of delayed effects.

2.4. Analysis of delayed reproductive death and giant cell formation

Cells were trypsinized and counted using a cell counter (Microcell Counter, Sysmex Co. Ltd., Tokyo). Aliquots of 10^2 cells were plated onto 100-mm dishes and incubated for 14 days before they were fixed with ethanol and then stained with 3% Giemsa. Colonies of more than 50 cells were counted. The cells, which occupied an area in the colony several times greater than the rest of the cells, were considered to be giant cells, as described previously [29].

2.5. Analysis of senescence-like growth arrest

Senecence-like growth arrest was examined by senescence-associated β-galactosidase (SA-β-gal) staining. Cells were washed briefly in PBS and fixed with 2% formaldehyde containing 0.2% glutaraldehyde for 5 min at room temperature. Then, the cells were washed extensively in PBS and incubated in SA-β-gal staining solution (40 mM citric acid/sodium phosphate, pH 6.0, 5 mM potassium ferrocyanide, 5 mM potassium ferricyanide, 150 mM NaCl, 2 mM $MgCl_2$) containing 1 mg/ml 5-bromo-4-chloro-3-indolyl β-D-galactopyranoside (X-gal), as described previously [30].

2.6. Analysis of delayed chromosomal instability

Exponentially growing cells were treated with 0.033 μg/ml Colcemid (GIBCO, Grand Island, NY) for 1 h, and mitotic cells were collected. The mitotic cells were treated with 0.075 M potassium chloride for 20 min, fixed in ice-cold Carnoy's fixative (methanol:acetic acid, 3:1) for 30 min, and spread on slide glasses using an air-drying method. After these cells were stained with 3% Giemsa, chromosome aberrations were classified as previously described [31]. Three independent experiments were performed, and more than 400 metaphases were counted for each sample.

2.7. Determination of oxidative stress in long-term culture

Oxidative stress was evaluated using DCFH fluorescence [32]. A part of the confluent cell cultures and cells cultured for 3 and 7 days at a low density were kept on ice, washed once with PBS, and then treated with 1 μM DCFH-DA (Molecular Probes) for 30 min. The cells were washed with PBS, and fluorescence intensity was measured using a fluorescence spectrophotometer F2000 (Hitachi, Tokyo, Japan). The excitation and emission wavelengths were 503 nm and 524 nm, respectively.

2.8. Statistical analysis

The data were analyzed statistically using Wilcoxon test.

3. Results

3.1. Rare cell division in a confluent culture

In order to maintain the cells at a confluent state, control cells (1×10^7) were subcultured in T75 flasks (Fig. 2). These cells underwent only one to two cell doublings within one passage. However, in X-irradiated population, some fractions of cells were expected to lose their proliferative potential, as the clonogenic surviving fraction of 4 Gy of X-rays was approximately 0.05. While no significant cell loss by apoptosis was observed, some giant cells caused by X-ray-induced senescence-like growth arrest were observed, as they were positive for SA-β-gal staining. Thus, such giant cells might be gradually eliminated from a population, most of the irradiated population contained cells that had lost proliferative potential. Therefore, the population doubling numbers (PDNs) at early passages (Fig. 3) might have been underestimated. Fresh medium was supplied every 3 or 4 days, and the cells were subcultured every 2 (first 12 months) or 3 (12–24 months) months. The cultures were trypsinized, and 1×10^7 cells were reseeded to maintain confluent cultures. As shown in Fig. 3, the total PDN of the control and 4 Gy-irradiated cells at 24 months was about 18.

3.2. Delayed induction of DNA damage

Twelve and twenty-four months after irradiation, cells were collected by trypsinization, and a portion of both the control and X-irradiated cells were cultured at low density for 3 and 7 days

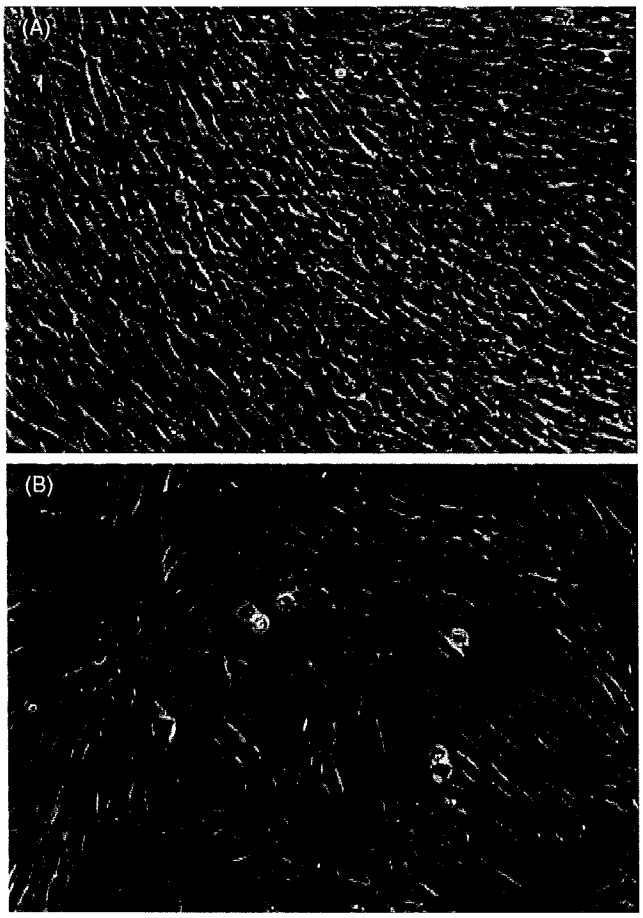

Fig. 2. Morphology of normal human diploid cells cultured in different conditions. (A) Confluent 4 Gy-irradiated cells cultured for 12 months, (B) a portion of 4 Gy-irradiated cells cultured at confluence for 12 months, reseeded at a low cell density.

to analyze delayed induction of DNA damage. In addition, colonies formed by the control and irradiated populations were independently isolated, and clonal cells were cultured to analyze the induction of delayed DNA damage. The cells were fixed and stained with an antibody recognizing phosphorylated ATM, i.e., the active form of ATM protein (Fig. 4). Because phosphorylated ATM forms discrete foci at sites of DNA double strand breaks, we determined

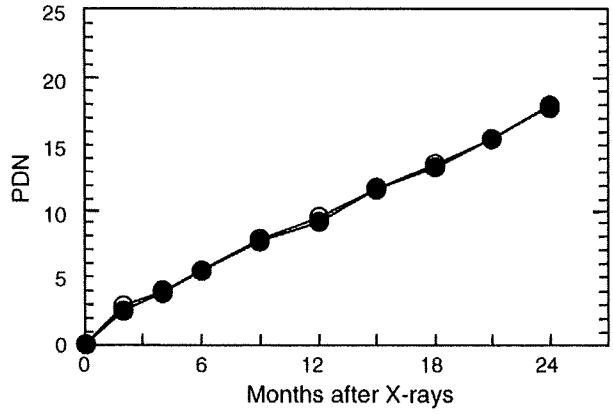

Fig. 3. Population doubling numbers of control and 4 Gy-irradiated cells cultured at confluence. Control (open circles) and 4 Gy-irradiated (closed circles) cells maintained at confluence were subcultured every 2 or 3 months, and the population doubling numbers were calculated as described in Section 2.

the number of foci in order to estimate the delayed induction of DNA double strand breaks in 10^3 cells. While phosphorylated ATM foci were rarely detected in the control cells (0.013 foci/cell), the number of such foci was significantly higher ($p < 0.05$) in cells derived from the exposed confluent cultures (Table 1). The frequency of phosphorylated ATM foci did not significantly differ between cells cultured for 3 and 7 days, indicating a similar probability of genomic instability in proliferating cells, irrespective of the number of days in culture. Because it is possible that observed DNA damage was due to the initial damage that had occurred when cells were irradiated, the frequency of phosphorylated ATM foci was also determined in cells clonally expanded after long-term quiescence. As shown in Table 2, no increase in the number of phosphorylated ATM foci was observed in any of the clones derived from irradiated population, as radiation-induced genomic instability is expressed randomly among the progenies of surviving cells. However, a higher number of clones with an increased frequency of foci were observed in irradiated clones as opposed to the non-irradiated clones. This finding clearly indicated that delayed DNA damage did occur when quiescent cells were forced to proliferate.

3.3. *Delayed induction of reproductive cell death, giant cells and chromosomal instability*

Delayed reproductive cell death, as determined by decreased colony-forming ability, was also apparent in cells from the exposed cultures (Table 3). In addition, the delayed induction of giant cells was more frequent in colonies formed by irradiated cells (Table 4). As shown in Table 5, the cells subcultured for 3 and 7 days also showed delayed induction of chromosomal aberrations. The frequency of every type of aberration was higher in the exposed cells that in the non-irradiated cells. The induction of chromatid-type aberrations as well as unstable chromosomal aberrations such as dicentric and ring chromosomes, indicates that delayed chromosome rearrangements occurred only after the confluent cells were forced to proliferate. In addition, the appearance of such non-clonal and multiple aberrations demonstrates that delayed chromosome instability was induced in those cells derived from exposed cultures that had been maintained in a quiescent state for a long period of time after irradiation.

3.4. *Determination of oxidative stress in long-term culture*

Levels of oxidative stress were evaluated using DCFH fluorescence (Fig. 5). While X-irradiation immediately and directly induced a significant increase in fluorescence intensity, there were no significant increases in ROS levels in the exposed cells after they had been maintained in a confluent state for a long period of time. It is possible that ROS levels increased in cells seeded at a low density. Therefore, cells cultured for 3 and 7 days at a low density were also examined; once again, no significant increases in ROS levels were observed in these latter two groups.

4. Discussion

It is well established that ionizing radiation can induce genomic instability in the progeny of irradiated cells. However, most studies conducted thus far have utilized replicating cells. Here, we demonstrated persist genomic instability for up to 24 months in quiescent normal human diploid cells. It was of interest that the incidence of delayed phenotypes was almost the same in cells cultured for 12 and 24 months, indicating that radiation-induced genomic instability was comparably maintained in quiescent cultures. These results are in disagreement with those showing that radiation-induced

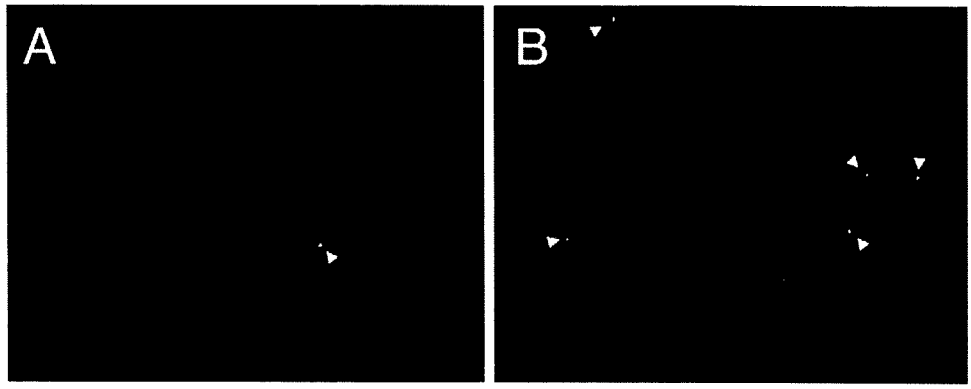

Fig. 4. Phosphorylated ATM foci in cells derived from confluent cultures maintained for 12 months. A portion of cells from control (A) and 4 Gy-irradiated (B) confluent cultures was grown at a low cells density. Cells were stained with anti-phosphorylated ATM antibody as described in Section 2. Phosphorylation of ATM is detected with Alexa-488-labelled secondary antibody (green), and chromosomal DNA is counterstained with DAPI (blue). Triangles indicate the foci-positive nuclei.

genomic instability gradually disappeared in normal proliferating human cells [33]. Notably, gradual disappearance of genomic instability was not observed in p53-defective cells. For example, unstable clones isolated from Chinese hamster cells retained their genomic instability for over 45 population doublings [34]. Furthermore, we previously observed that the delayed activation of a DNA damage checkpoint in the progeny of p53-defective human tumor cells surviving radiation exposure [35]. Thus, it can be concluded that in proliferating normal cells, in which DNA damage response is intact, initially unstable cells are gradually eliminated by delayed reproductive cell death or by apoptosis. The absence of growth-related cell death in quiescent cells could maintain a state of genomic instability for a long period of time after irradiation.

It should be mentioned that radiation-induced genomic instability has not been commonly observed in the previous studies using normal human cells. For example, Dugan and Bedford reported finding no evidence for the induction of such instability, although they observed a senescence-related chromosomal instability in the progeny of both irradiated and unirradiated cells [36]. Such senescence-related changes were also observed in the current study. For example, as shown in Table 4, the frequency of dicentric chromosomes was higher in cells cultured for 24 months, which might be due to shortened telomeres. The reason for this discrepancy remains unknown; here, we attempt to use cells from early passages in order to avoid the possibility that senescence-related changes mask persistent radiation effects. In the present study, we confirmed the significant induction of genomic instability only in the progeny of irradiated cells. Therefore, these results indicate that the observed genomic instability in quiescent cells is indeed dependent on irradiation.

Recently, several studies have proposed the importance of tissue stem cells as targets for carcinogenesis [14–17]. In contrast to the somatic cells that divide continuously, tissue stem cells stay quiescent in a stem cell niche [18–21]. Although we did not use stem cells in this study, radiation-induced genomic instability is likely to persist over the lifetime of quiescent cells such as those found in niche. Such persistent inheritance of radiation-induced genomic instability in stem cells was well-described in mice [10], and has been suggested in exposed humans [25,26,37,38]. Conditions enforcing cell division (e.g., tissue damage caused by radiation exposure) could provide opportunities for quiescent stem cells to manifest radiation-induced genomic instability.

The mechanism(s) underlying the perpetuation of genomic instability in quiescent cells remains to be determined. To date, elevated ROS levels have been considered as a cause of persisted instability [39–44]. Recent *in vivo* studies have suggested that inflammatory-type tissue response provides microenvironment that leads to persistent genomic instability [42]. Moreover, it has been shown that dysfunctional mitochondria are involved in the persistence of radiation-induced genomic instability [39–44]. Thus, it is reasonable to consider that persistent oxidative stress is among the mechanisms associated with radiation-induced genomic instability. We, therefore, examined ROS levels using DCFH fluorescence in irradiated quiescent cells. Although direct ROS production was

Table 1
Delayed induction of phospho-ATM foci.

Cells	Total no. of cells counted	% cells with foci	No. of foci per cell ($\times 10^{-2}$)
12 months after X-rays			
3 days			
0 Gy	1000	1.3 ± 0.6	1.3 ± 0.6*
4 Gy	1000	5.0 ± 0.2	7.0 ± 2.0*
7 days			
0 Gy	1000	1.5 ± 0.7	1.5 ± 0.7*
4 Gy	1000	5.3 ± 0.3	7.5 ± 2.2*
24 months after X-rays			
3 days			
0 Gy	1000	1.7 ± 0.6	2.7 ± 1.2**
4 Gy	1000	7.0 ± 0.2	9.3 ± 3.5**
7 days			
0 Gy	1000	1.6 ± 0.6	2.8 ± 1.4**
4 Gy	1000	6.9 ± 0.5	9.5 ± 3.7**

* $p < 0.01$.
** $p < 0.05$.

Table 2
Delayed induction of phospho-ATM foci in isolated colonies.

Cells	Total no. of cells counted	% cells with foci	No. of foci/cell ($\times 10^{-2}$)	Cells	Total no. of cells counted	% cells with foci	No. of foci/cell ($\times 10^{-2}$)
12 months after X-rays							
C1	1000	1.3	1.3	X1	1000	4.3	7.3
C2	1000	1.2	1.2	X2	1000	1.0	1.3
C3	1000	1.0	1.3	X3	1000	1.3	1.9
C4	1000	1.1	1.5	X4	1000	1.2	1.7
C5	1000	1.2	1.3	X5	1000	1.1	1.6
C6	1000	1.3	1.3	X6	1000	4.5	6.3
C7	1000	1.1	1.1	X7	1000	7.3	11.9
C8	1000	1.0	1.5	X8	1000	1.1	1.3
C9	1000	1.0	1.8	X9	1000	1.2	3.3
C10	1000	1.3	1.9	X10	1000	1.3	4.1
C11	1000	1.5	1.5	X11	1000	6.3	9.2
C12	1000	1.9	1.9	X12	1000	3.1	4.8
C13	1000	1.1	1.4	X13	1000	3.3	6.9
C14	1000	1.0	1.3	X14	1000	2.3	3.1
C15	1000	1.1	1.3	X15	1000	1.2	1.5
C16	1000	1.1	1.4	X16	1000	9.3	14.5
C17	1000	1.3	1.7	X17	1000	1.0	1.3
C18	1000	1.7	2.1	X18	1000	1.1	1.1
C19	1000	1.5	1.8	X19	1000	3.3	4.3
C20	1000	1.7	1.9	X20	1000	1.9	2.0
24 months after X-rays							
C1	1000	1.1	1.3	X1	1000	5.3	11.3
C2	1000	1.3	1.7	X2	1000	4.2	6.1
C3	1000	1.5	1.9	X3	1000	3.3	5.0
C4	1000	1.7	2.1	X4	1000	2.9	4.3
C5	1000	1.2	1.8	X5	1000	1.5	1.9
C6	1000	1.3	1.5	X6	1000	1.3	3.3
C7	1000	1.3	1.8	X7	1000	1.1	1.7
C8	1000	1.0	1.9	X8	1000	1.0	2.8
C9	1000	1.1	2.0	X9	1000	7.3	13.3
C10	1000	1.0	1.3	X10	1000	7.2	8.3
C11	1000	1.2	1.8	X11	1000	9.3	11.0
C12	1000	1.4	1.9	X12	1000	4.0	5.3
C13	1000	1.3	1.5	X13	1000	1.1	1.8
C14	1000	1.7	2.6	X14	1000	3.7	5.3
C15	1000	1.2	2.7	X15	1000	2.3	3.3
C16	1000	1.1	1.7	X16	1000	1.0	2.0
C17	1000	1.3	1.5	X17	1000	4.7	7.7
C18	1000	1.0	1.8	X18	1000	5.3	10.5
C19	1000	1.1	1.8	X19	1000	7.1	6.7
C20	1000	1.2	1.7	X20	1000	1.8	3.1

observed immediately after irradiation, no increases were observed in ROS levels of quiescent cells cultured for a long period of time after irradiation. We also examined ROS levels in cells forced to proliferate for 3 and 7 days at a low cell density. However, neither of these groups showed increased levels of ROS. Thus, our results clearly indicated that ROS-independent mechanism can contribute to the perpetuation of radiation-induced genomic instability. As we reported previously, X-ray-induced large deletions potentially cause unstable chromosome regions (PUCRs), which could be transmitted through generations [9,45]. These deletions are not DNA breaks by themselves, but abnormal structures in higher-order chromatin created through mis-rejoining of DNA double strand breaks. Such structural radiation signature may mediate perpetuation of genomic instability in quiescent cells.

In summary, the present study demonstrated that X-irradiation induces genomic instability in normal quiescent human diploid cells, and this instability persists for up to 24 months after irradiation. These findings indicated that ROS-independent mechanisms "memorize" initial DNA damage, and are somehow associated with radiation-induced genomic instability. As no delayed phenotypes accumulate in the quiescent cells observed here, such a DNA damage memory is most likely to induce delayed DNA breakage, which result in the induction of delayed phenotypes, only after quiescent cells are exposed to a condition that initiate cell proliferation.

Table 3
Delayed reproductive death.

Cells	Cloning efficiencies (%)
12 months after X-rays	
0 Gy	32.7 ± 1.5*
4 Gy	17.0 ± 2.0*
24 months after X-rays	
0 Gy	10.7 ± 0.6*
4 Gy	4.0 ± 1.0*

* $p < 0.01$.

Table 4
Delayed induction of giant cells.

Cells	No. of colonies with giant cells/no. of colonies counted (%)
12 months after X-rays	
0 Gy	9/264 (0.034)*
4 Gy	44/228 (0.193)*
24 months after X-rays	
0 Gy	13/320 (0.041)*
4 Gy	19/220 (0.086)*

* $p < 0.01$.

Table 5
Induction of delayed chromosomal instability.

Cells	No. of cells counted	No. of metaphases with aberrations (%)	No. of aberrations				
			Dic (with Frag)	Gaps	Breaks	Fragments	Ring
12 months after X-rays							
3 days							
0 Gy	418	7 (1.7)*	0	3	2	2	0
4 Gy	402	44 (10.9)*	12 (12)	20	12	15	0
7 days							
0 Gy	513	7 (1.4)*	0	2	3	2	0
4 Gy	472	52 (11.0)*	10 (10)	25	13	4	0
24 months after X-rays							
3 days							
0 Gy	500	17 (3.4)*	3 (1)	7	7	3	0
4 Gy	652	86 (13.2)*	34 (13)	34	22	20	9
7 days							
0 Gy	515	19 (3.7)*	3 (3)	8	7	4	0
4 Gy	635	81 (12.8)*	27 (19)	27	15	7	5

* $p < 0.01$.

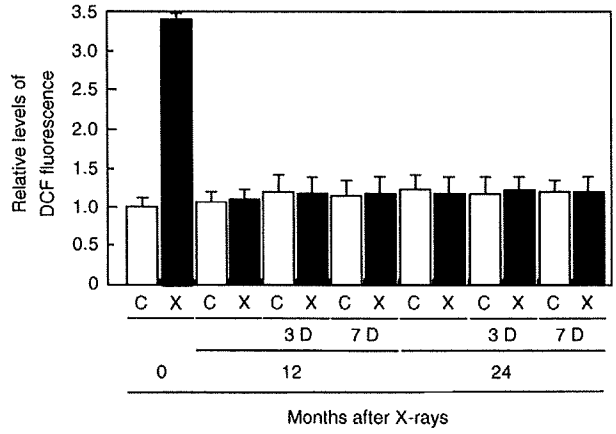

Fig. 5. Oxidative levels determined by DCFH fluorescent assay. Portions of both control (open bars) and 4 Gy-irradiated (closed bars) confluent cultures maintained for 12 and 24 months were treated with 1 μM DCFH-DA for 30 min. In addition, cells cultured for 3 days (3D) and 7 days (7D) at a low density were treated with 1 μM DCFH-DA for 30 min. Fluorescence intensity was determined by a fluorescence spectrophotometer as described in Section 2.

Conflict of interest

None.

Acknowledgements

This work was supported in part by Grants-in-Aid for scientific research and by the Global COE program from the Japanese Ministry of Education, Culture, Sports, Science, and Technology of Japan.

References

[1] W.F. Morgan, Non-targeted and delayed effects of exposure to ionizing radiation. I. Radiation-induced genomic instability and bystander effects in vitro, Radiat. Res. 159 (2003) 567–580.
[2] W.F. Morgan, Non-targeted and delayed effects of exposure to ionizing radiation. I. Radiation-induced genomic instability and bystander effects in vivo, clastpgenic factors and transgenerational effects, Radiat. Res. 159 (2003) 581–596.
[3] J.B. Little, Cellular radiation effects and the bystander effects, Mutat. Res. 597 (2006) 113–118.
[4] C. Mothersill, C. Seymour, Radiation-induced bystander effects and the DNA paradigm: an "out of field" perspective, Mutat. Res. 579 (2006) 5–10.
[5] E.G. Wright, P.J. Coates, Untargeted effects of ionizing radiation: implications for radiation pathology, Mutat. Res. 597 (2006) 119–132.
[6] W.F. Morgan, J.P. Day, M.I. Kaplan, E.M. McGhee, C.L. Limoli, Genomic instability induced by ionizing radiation, Radiat. Res. 146 (1996) 247–258.
[7] J.B. Little, Genomic instability and bystander effects: a historical perspective, Oncogene 22 (2003) 6978–6987.
[8] S.A. Lorimore, P.J. Coates, E.G. Wright, Radiation-induced genomic instability and bystander effects: inter-related nontargeted effects of exposure to ionizing radiation, Oncogene 22 (2003) 7058–7069.
[9] K. Suzuki, M. Ojima, S. Kodama, M. Watanabe, Radiation-induced DNA damage and delayed induced genomic instability, Oncogene 22 (2003) 6988–6993.
[10] M.A. Kadhim, D.A. MacDonald, D.T. Goodhead, S.A. Lorimore, S.J. Marsden, E.G. Wright, Transmission of chromosomal instability after plutonium alpha-particle irradiation, Nature 355 (1992) 738–740.
[11] K. Suzuki, Multistep nature of X-ray-induced neoplastic transformation in mammalian cells: genetic alteration and instability, J. Radiat. Res. 38 (1997) 55–63.
[12] L. Huang, A.R. Snyder, W.F. Morgan, Radiation-induced genomic instability and its implications for radiation carcinogenesis, Oncogene 22 (2003) 5848–5854.
[13] O. Niwa, Induced genomic instability in irradiated germ cells and in the offspring; reconciling discrepancies among the human and animal studies, Oncogene 22 (2003) 7078–7086.
[14] E. Fuchs, J.A. Segre, Stem cells: a new lease on life, Cell 100 (2002) 143–155.
[15] T. Reya, S.J. Morrison, M.F. Clarke, I.L. Weissman, Stem cells, cancer, and cancer stem cells, Nature 414 (2001) 105–111.
[16] R. Pardal, M.F. Clarke, S.J. Morrison, Applying the principal of stem-cell biology to cancer, Nat. Rev. Cancer 3 (2003) 895–902.
[17] J.E. Visvader, G.J. Lindeman, Cancer stem cells in solid tumours: accumulating evidences and unresolved questions, Nat. Rev. Cancer 8 (2008) 755–768.
[18] E. Fuchs, T. Tumbar, G. Guasch, Socializing with the neighbors: stem cells and their niche, Cell 116 (2004) 769–778.
[19] L. Li, W.B. Neaves, Normal stem cells and cancer stem cells: the niche matters, Cancer Res. 66 (2006) 4553–4557.
[20] K.A. Moore, I.R. Lemischka, Stem cells and their niche, Science 311 (2006) 1880–1885.
[21] D.T. Scadden, The stem-cell niche as an entity of action, Nature 441 (2006) 1075–1079.
[22] F. Arai, T. Suda, Maintenance of quiescent hematopoietic stem cells in the osteoblastic niche, Ann. N.Y. Acad. Sci. 1106 (2007) 41–53.
[23] S. Bao, R.E. McLendon, Y. Hao, Q. Shi, A.B. Hjelmeland, M.W. Dewhirst, D.D. Bigner, J.N. Rich, Glioma stem cells promote radioresistance by preferential activation of the DNA damage response, Nature 444 (2006) 756–760.
[24] M. Baumann, M. Krause, R. Hill, Exploring the role of cancer stem cells in radioresistance, Nat. Rev. Cancer 8 (2008) 545–554.
[25] D.L. Preston, E. Ron, S. Tokuoka, S. Funamoto, N. Nishi, M. Soda, K. Mabuchi, K. Kodama, Solid cancer incidence in atomic bomb survivors: 1958–1989, Radiat. Res. 168 (2007) 1–64.
[26] D. Pawel, D. Preston, D. Pierce, J. Cologne, Improved estimates of cancer site-specific risks for A-bomb survivors, Radiat. Res. 169 (2008) 87–98.
[27] M. Watanabe, M. Suzuki, K. Suzuki, K. Nakano, K. Watanabe, Effect of multiple irradiation with low doses of gamma-rays on morphological transformation and growth ability of normal human embryo cells in vitro, Int. J. Radiat. Biol. 62 (1992) 711–718.
[28] K. Suzuki, H. Okada, M. Yamauchi, Y. Oka, S. Kodama, M. Watanabe, Qualitative and quantitative analysis of phosphorylated ATM foci induced by low-dose ionizing radiation, Radiat. Res. 165 (2006) 499–504.
[29] K. Suzuki, R. Takahara, S. Kodama, M. Watanabe, In situ detection of chromosome bridge formation and delayed reproductive death in normal human embryonic cells surviving X-irradiation, Radiat. Res. 150 (1998) 375–381.
[30] G.P. Dimri, X. Lee, G. Basile, M. Acosta, G. Scott, C. Roskelley, E.E. Medrano, M. Linskens, I. Rubelj, J. Campici, A biomarker that identifies senescent human

cells in culture and in aging skin in vivo, Proc. Natl. Acad. Sci. U.S.A. 92 (1995) 9363–9367.
[31] J.R. Savage, Classification and relationships of induced chromosomal structural changes, J. Med. Genet. 13 (1976) 103–122.
[32] G. Kashino, K.M. Prise, K. Suzuki, N. Matsuda, S. Kodama, M. Suzuki, K. Nagata, Y. Kinashi, S.-I. Masunaga, K. Ono, M. Watanabe, Effective suppression of bystander effects by DMSO treatment of irradiated CHO cells, J. Radiat. Res. 48 (2007) 327–333.
[33] K. Roy, S. Kodama, K. Suzuki, M. Watanabe, Delayed cell death, giant cell formation and chromosome instability induced by X-irradiation in human embryo cells, J. Radiat. Res. 40 (1999) 311–322.
[34] W.P. Chang, J.B. Little, Delayed reproductive death in X-irradiated Chinese hamster ovary cells, Int. J. Radiat. Biol. 60 (1991) 483–496.
[35] K. Suzuki, S. Yokoyama, S. Waseda, S. Kodama, M. Watanabe, Delayed reactivation of p53 in the progeny of cells surviving ionizing radiation, Cancer Res. 63 (2003) 936–941.
[36] L.C. Dugan, J.S. Bedford, Are chromosomal instabilities induced by exposure of cultured normal human cells to low- or high-LET radiation? Radiat. Res. 159 (2003) 301–311.
[37] N. Kamada, K. Tanaka, N. Oguma, K. Mabuchi, Cytogenetic and molecular changes in leukemia among atomic bomb survivors, J. Radiat. Res. 32 (1991) 257–265.
[38] M.P. Hande, T.V. Azizova, C.R. Geard, L.E. Burak, C.R. itchell, V.F. Khokhryakov, E.K. Vasilenko, D.J. Brenner, Past exposure to densely ionizing radiation leaves a unique permanent signature in the genome, Am. J. Hum. Genet. 72 (2003) 1162–1170.
[39] E.I. Azzam, S.M. de Toledo, J.B. Little, Oxidative metabolism, gap junctions and the ionizing radiation-induced bystander effect, Oncogene 22 (2003) 7050–7057.
[40] C.L. Limoli, E. Giedzinski, W.F. Morgan, S.G. Swarts, G.D. Jones, W. Hyun, Persistent oxidative stress in chromosomally unstable clones, Cancer Res. 63 (2003) 3107–3111.
[41] G.J. Kim, G.M. Fiskum, W.F. Morgan, A role for mitochondrial dysfunction in perpetuating radiation-induced genomic instability, Cancer Res. 66 (2006) 10377–10383.
[42] E.G. Wright, Microenvironment and genetic factors in haemopoietic radiation responses, Int. J. Radiat. Biol. 83 (2007) 813–818.
[43] P.J. Coates, J.K. Rundle, S.A. Lorimore, E.G. Wright, Indirect macrophage responses to ionizing radiation: implications for genotype-dependent bystander signaling, Cancer Res. 68 (2008) 450–456.
[44] J.H. Miller, S. Jin, W.F. Morgan, A. Yang, Y. Wan, U. Aypar, J.S. Peters, D.L. Springer, Profiling mitochondrial proteins in radiation-induced genome-unstable cell lines with persistent oxidative stress by mass spectrometry, Radiat. Res. 169 (2008) 700–706.
[45] H. Toyokuni, A. Maruo, K. Suzuki, M. Watanabe, The contribution of radiation-induced large deletion of the genome to chromosomal instability, Radiat. Res. 171 (2009) 198–203.

Mutation Research 683 (2010) 29–34

Contents lists available at ScienceDirect

Mutation Research/Fundamental and Molecular Mechanisms of Mutagenesis

journal homepage: www.elsevier.com/locate/molmut
Community address: www.elsevier.com/locate/mutres

Role of Ku80-dependent end-joining in delayed genomic instability in mammalian cells surviving ionizing radiation

Keiji Suzuki[a,*], Seiji Kodama[c], Masami Watanabe[b]

[a] Course of Life Sciences and Radiation Research, Graduate School of Biomedical Sciences, Nagasaki University, 1-12-4 Sakamoto, Nagasaki 852-8523, Japan
[b] Kyoto University Research Reactor Institute, Kumatori-cho Sennan-gun, Osaka 590-0494, Japan
[c] Research Institute for Advanced Science and Technology, Osaka Prefecture University, 1-2 Gakuen-machi, Sakai 599-8570, Japan

ARTICLE INFO

Article history:
Received 9 June 2009
Received in revised form
17 September 2009
Accepted 2 October 2009
Available online 12 October 2009

Keywords:
Ionizing radiation
Genomic instability
DNA repair
Chromosome aberration
Non-homologous end-joining
CHO

ABSTRACT

Ionizing radiation induces delayed destabilization of the genome in the progenies of surviving cells. This phenomenon, which is called radiation-induced genomic instability, is manifested by delayed induction of radiation effects, such as cell death, chromosome aberration, and mutation in the progeny of cells surviving radiation exposure. Previously, there was a report showing that delayed cell death was absent in Ku80-deficient Chinese hamster ovary (CHO) cells, however, the mechanism of their defect has not been determined. We found that delayed induction of DNA double strand breaks and chromosomal breaks were intact in Ku80-deficient cells surviving X-irradiation, whereas there was no sign for the production of chromosome bridges between divided daughter cells. Moreover, delayed induction of dicentric chromosomes was significantly compromised in those cells compared to the wild-type CHO cells. Reintroduction of the human Ku86 gene complimented the defective DNA repair and recovered delayed induction of dicentric chromosomes and delayed cell death, indicating that defective Ku80-dependent dicentric induction was the cause of the absence of delayed cell death. Since DNA-PKcs-defective cells showed delayed phenotypes, Ku80-dependent illegitimate rejoining is involved in delayed impairment of the integrity of the genome in radiation-survived cells.

1. Introduction

It is generally accepted that DNA repair pathways are indispensable for the survival of cells exposed to DNA damaging agents, such as ionizing radiation [1–5]. However, DNA repair, by itself, may threaten the stability of the genome in the cells surviving DNA damaging agents [6–9]. For example, non-homologous end-joining (NHEJ), which is the primary DNA repair pathway functions in G1 phase, is error-prone. It sometimes causes loss or rearrangement of the genetic information through mis-rejoining of DNA double strand breaks. Processing of DNA broken ends by exonucleases and endonucleases also provide another chance to alter DNA sequences. These events result in a loss of heterozygosity as well as gross genome rearrangements. In contrast, homologous recombination is a faithful repair in general, as homologous sister chromatids are used to restore the gap of the genetic information. Although most genome rearrangements are generated directly by the initial radiation exposure [10], recent findings have demonstrated that the integrity of the genome is also endangered eventually, if the cells were survived exposure to DNA damaging agents.

It is well described that ionizing radiation induces delayed effects in the progeny of surviving cells [11–14]. This phenomenon is now called radiation-induced genomic instability, which is manifested as the expression of various delayed effects, such as delayed reproductive death or lethal mutation, delayed chromosomal instability, and delayed mutagenesis in the progenies of cells surviving radiation. Radiation-induced genomic instability results in accumulating gene mutations and chromosomal rearrangements, therefore, it has been thought to play a pivotal role in radiation-induced carcinogenesis [15–18]. Because radiation-induced genomic instability is induced in a certain fraction of the progenies stem from a single survived cell, not a single gene mutation but some epigenetic changes may be involved in the initiation of radiation-induced genomic instability. Although oxidative stress and altered chromatin structure have been proposed as the mechanisms of perpetuation of radiation-induced genomic instability [19–24], the mechanism of manifestation has not been fully understood yet. We have shown that delayed unscheduled induction of DNA double strand breaks is involved in the manifestation of delayed phenotypes [25]. In fact, our previous study indicated that increased phosphorylated histone H2AX foci, which correspond to DNA double strand breaks, are frequently detected in the progeny of normal human diploid cells surviving X-rays. Moreover, delayed reactivation of p53 in response to DNA damage was manifested in

* Corresponding author.
E-mail address: kzsuzuki@nagasaki-u.ac.jp (K. Suzuki).

0027-5107/$ – see front matter © 2009 Elsevier B.V. All rights reserved.
doi:10.1016/j.mrfmmm.2009.10.003

the surviving clones [25]. Delayed induction of DNA double strand breaks was also confirmed by delayed induction of chromosomal aberrations [26]. Thus, it is evidenced that induction of DNA double strand breaks is induced indirectly in surviving cells from exposure to radiation, suggesting that DNA repair pathways could play roles in protecting the genome of surviving cells from harmful effects of radiation.

Previously, Chang and Little reported that radiation-induced genomic instability was abrogated in xrs5 cells, which are NHEJ-deficient Chinese hamster cells defective in Ku80 protein [27]. It was found that delayed reproductive death was not observed in these cells, however, the reason for the absence of delayed reproductive death in xrs5 cells has not been elucidated yet. We have hypothesized that defective NHEJ in xrs5 cells decreases the chance of mis-rejoining of the broken ends, which result in the formation of dicentric chromosomes involved in division halt. Therefore, we examined delayed chromosomal instability in two NHEJ-defective cells, xrs5 and xrs6 cells, and compared the frequency with the wild-type CHO cells. Firstly, we found that delayed induction of DNA double strand breaks in those cells, determined by DNA repair foci formation, was similar. Furthermore, delayed induction of chromatid breaks showed no defect in Ku80-deficient cells. However, delayed induction of dicentric chromosomes was significantly compromised in both xrs5 and xrs6 cells. These results demonstrate that Ku80-dependent mechanism is involved in delayed induction of dicentric chromosomes, and that dicentric chromosomes caused by the mis-rejoining of broken ends are associated with the induction of delayed cell death through the inhibition of cell division. This conclusion was confirmed by the experiment, in which the reintroduction of human Ku80 gene into xrs5 cells restored both delayed dicentric formation and delayed reproductive death. Furthermore, delayed induction of dicentric chromosomes was observed in cells defective in the catalytic subunit of DNA-dependent protein kinase (DNA-PKcs). In summary, our present study clearly indicates that the progenies of surviving cells induce delayed DNA damage several generations after the initial insult, and DNA repair capacity is an important determinant for the integrity of the genome in the cells surviving radiation exposure.

2. Experimental procedure

2.1. Cell culture and irradiation

Chinese hamster ovary (CHO) cells, XRCC1-defective EM-9 cells, and Ku80-defective xrs5 and xrs6 cells were cultured in αMEM supplemented with 10% fetal bovine serum (FBS) (TRACE Bioscience PTY Ltd., Australia). Severe combined immunodeficiency (*Scid*) mouse (C.B-17 *scid/scid*) and isogenic wild-type mouse (C.B-17 +/+) embryonic fibroblasts were cultured in DMEM supplemented with 10% FBS [28]. Embryonic fibroblasts from C3H/He wild-type mouse and $ATM^{-/-}$ knockout mouse were cultured in DMEM supplemented with 10% FBS [29]. The human KU86 gene was introduced into xrs5 cells by electroporation, and the cells were cultured in αMEM containing 200 μg/ml of G418 and 10% fetal bovine serum (TRACE Bioscience PTY Ltd., Australia). Exponentially growing cells were irradiated with X-rays from an X-ray generator at 150 kVp and 5 mA with a 0.1-mm copper (SOFTEX M-150WE, Softex, Osaka). The dose rate was 0.44 Gy/min. Dose rates were determined with an ionization chamber.

2.2. Cell survival

Cell survival was determined by colony formation assay. Cells cultured in T25 flasks were irradiated with various doses of X-rays, collected by trypsinization, counted the cell number, and appropriate numbers of cells, which give 10^2 surviving cells, were seeded into at least three 100-mm dishes. The cultures were incubated in a CO_2 incubator for 10 days before fixation with ethanol. The colonies were stained with Giemsa's solution, and those consisting more than 50 cells were counted.

2.3. Analysis of delayed effects

Cells cultured in T25 flasks were irradiated with various doses of X-rays. CHO cells were irradiated with 8 and 10 Gy of X-rays, while xrs5 and xrs6 cells were irradiated with 2 and 4 Gy. EM-9 cells were irradiated with 6 and 8 Gy of X-rays. After irradiation, the irradiated cells and the control cells were collected by trypsinization, and appropriate numbers of cells, which give 10^2 surviving cells, were seeded into ten 100-mm dishes. Ten days after irradiation, the primary colonies formed in ten independent dishes were collected by trypsinization. The number of cells was counted, and total population doubling levels (PDLs) were calculated by using the total numbers of cells in ten dishes divided by the number of colonies formed in ten dishes. They were used as the cells at 15–20 population doublings. Rest of the cells was used for the secondary colony formation, and 10^2 cells were re-inoculated into another ten 100-mm dishes. After 10 days, all the colonies formed in ten dishes were collected by trypsinization, counted the number of cells, and total population doubling levels were calculated. They were used as the cells at 30–35 population doublings after irradiation.

2.4. Detection of giant cells and delayed chromosomal bridge formation

Exponentially growing cells were plated onto 22 mm × 22 mm coverslips, and incubated for 24 h before fixation with methanol. Then, cells were stained with 5% Giemsa's solution. The cells, which occupied an area in the colony several times greater than the rest of the cells, were considered to be giant cells as described previously. Chromosomal bridges, which were detected between two dividing daughter nuclei in the anaphase cells, were counted.

2.5. Detection of delayed chromosomal aberrations

Exponentially growing cells were treated with 0.033 μg/ml colcemid (GIBCO, Grand Island, NY) for 1 h, and mitotic cells were collected. They were treated with 0.075 M potassium chloride for 20 min, fixed in ice-cold Carnoy's fixative (methanol:acetic acid, 3:1) for 30 min, and spread on slide glasses using an air-drying method. After staining with 3% Giemsa's solution, chromosome aberrations were classified as previously described [14]. Three independent experiments were performed, and total 200 metaphases were counted per each sample.

2.6. Detection of delayed DNA damage

Delayed induction of DNA double strand breaks was determined by 53BP1 foci. The cells cultured on coverslips were fixed with 4% formaldehyde, permeabilized with 0.5% Triton X-100, and then were washed extensively with phosphate buffered saline (PBS). The primary antibody, anti-53BP1 antibody (Bethyl laboratories Inc., TX), were diluted in 100 μl of TBS-DT (20 mM Tris–HCl, 137 mM NaCl, pH7.6, containing 50 mg/ml skim milk and 0.1% Tween-20), and applied on the cover slips. The samples were incubated for 2 h in a humidified CO_2 incubator at 37 °C. The primary antibody was washed with PBS, and Alexa594-labelled anti-rabbit IgG antibodies (Molecular Probes, Inc., OR) were added. The cover slips were incubated for 1 h in a humidified CO_2 incubator at 37 °C. They were then washed with PBS and counterstained with 0.1 mg/ml of DAPI. The samples were examined with an Olympus fluorescence microscope AX80 (Olympus, Tokyo). Digital images were captured by a Quantix 1400 camera (Photometrics, AZ), and the images were analyzed by IPLab Spectrum analysis software (Signal Analytics Corporation, VA).

2.7. Immunoblotting and detection

Exponentially growing cells were lysed in lysis buffer (50 mM Tris–HCl (pH7.2), 150 mM NaCl, 1% NP-40, 1% sodium deoxycholate, and 0.1% SDS) containing 1 mM 4-(2-aminoethyl)-benzensulfonyl fluoride hydrochloride. The cell lysate was sheared through 28 G needle 5 times and cleared by centrifugation at 15,000 rpm for 10 min at 4 °C, and then supernatant was used as total cellular protein. Total protein concentration was determined by the BCA protein assay (Pierce, Rockford, IL). Protein samples (16 μg) were electrophoresed on SDS-polyacrylamide gel and were electrophoretically transferred to a polyvinyl difluoride membrane in a transfer buffer (100 mM Tris, 192 mM glycine). After overnight incubation with blocking solution (10% skim milk), the membrane was incubated with anti-Ku80 monoclonal antibody (clone 111, KAMIYA Biomedical Co.) or anti-XRCC1 polyclonal antibody (NOVUS Biologicals), a biotinylated anti-mouse IgG antibody, and streptavidine–alkaline phosphatase. The bands were visualized after addition of nitroblue tetrazolium/5-bromo-4-chloro-3-indolyl phosphate as a substrate.

2.8. Data analysis

A Student's *t*-test was used to evaluate significant difference between the control and irradiated cells. *P* values of less than 0.05 were considered significant difference.

3. Results

Exponentially growing CHO, XRCC1-defective EM-9 cells, and Ku80-deficient xrs5 and xrs6 cells were exposed to various doses of X-irradiation. Both xrs5 and xrs6 cells show significant reduction of cell survival as compared to CHO cells (Fig. 1). In order to compare delayed induction of genomic instability at the same survival levels, 8 and 10 Gy of X-rays were irradiated to CHO, while 2 and 4 Gy

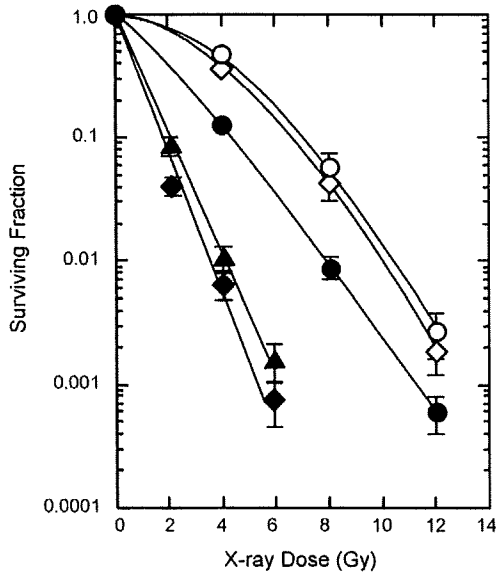

Fig. 1. Survival curves of CHO cells and Ku80-deficient cells. (○) CHO cells; (●) EM9 cells; (♦) xrs5 cells; (▲) xrs6 cells; (◊) xrs5 cells with the human KU86 gene.

of X-rays and 6 and 8 Gy of X-rays were exposed to xrs5 and xrs6 cells, and EM-9 cells, respectively. To compliment the defect in xrs5 cells, the human Ku86 gene was introduced by electroporation. As shown in Fig. 2, the introduced cells expressed significant amount of human KU80 protein, and as a result, radiation sensitivity was also complimented (Fig. 1).

Manifestation of radiation-induced genomic instability was determined by the expression of the delayed effects. As shown in Table 1, delayed reproductive death was completely absent in both xrs5 and xrs6 cells, whereas CHO and EM-9 cells showed decreased cloning efficiency. Induction of giant cells and delayed chromosomal bridges were also abrogated in xrs5 and xrs6 cells (Tables 1 and 2). In order to confirm that defective induction of these delayed phenotypes are caused by the simple Ku80-deficiency, the human Ku86 gene was introduced into xrs5 cells. It was confirmed that complementation of the defective Ku80 function in xrs5 cells simultaneously restored delayed reproductive death, giant cell formation and delayed chromosomal bridge formation to the levels observed in CHO cells. Thus, the results clearly indicated that Ku80-dependent rejoining is involved in manifesting delayed phenotypes in the progenies of X-ray-surviving cells.

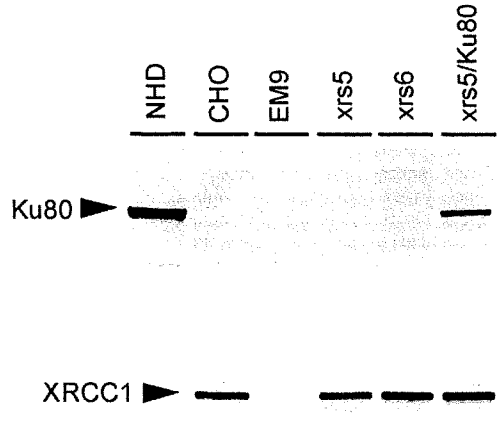

Fig. 2. Expression of Ku80 and XRCC1 in CHO and mutants. Total proteins were extracted from exponentially growing cells. Samples (16 μg) were subjected to western blot analysis probed with anti-Ku80 and XRCC1 antibodies. To check the expression of exogenous human Ku80 protein, total proteins from normal human diploid (NHD) cells were used.

Table 1
Cloning efficiency and frequency of giant cells at 30–35 PDL post-irradiation.

Cells	Cloning efficiencies (%)	% colonies with giant cells
CHO		
0 Gy	99.8 ± 12.6	7.0 ± 3.5
8 Gy	75.8 ± 11.6	15.1 ± 5.7
10 Gy	78.0 ± 10.2	21.4 ± 8.3
EM9		
0 Gy	79.0 ± 12.3	3.9 ± 1.4
6 Gy	70.5 ± 3.1	9.8 ± 3.6
8 Gy	65.5 ± 8.4	13.7 ± 3.5
xrs5		
0 Gy	63.0 ± 15.4	4.2 ± 2.5
2 Gy	61.0 ± 2.8	4.5 ± 1.9
4 Gy	64.0 ± 8.0	4.7 ± 3.1
xrs6		
0 Gy	57.5 ± 2.7	5.0 ± 3.3
2 Gy	54.3 ± 6.8	4.8 ± 3.5
4 Gy	58.3 ± 6.2	4.2 ± 3.9
xrs5/Ku80		
0 Gy	89.7 ± 10.4	6.5 ± 3.3
8 Gy	69.1 ± 9.6	12.0 ± 7.5
10 Gy	65.8 ± 11.4	17.8 ± 6.4

Table 2
Delayed chromosome bridge formation in mitotic cells at 30–35 PDL post-irradiation.

Cells	% cells with chromosome bridge
CHO	
0 Gy	2.6 ± 1.5
8 Gy	9.0 ± 4.1
10 Gy	15.3 ± 6.7
EM9	
0 Gy	3.8 ± 2.1
6 Gy	6.4 ± 3.4
8 Gy	16.0 ± 6.0
xrs5	
0 Gy	8.1 ± 4.4
2 Gy	8.2 ± 3.9
4 Gy	7.3 ± 3.1
xrs6	
0 Gy	13.0 ± 7.8
2 Gy	10.2 ± 7.4
4 Gy	9.3 ± 6.8
xrs5/Ku80	
0 Gy	4.8 ± 2.8
8 Gy	8.2 ± 7.3
10 Gy	14.3 ± 8.6

It is possible that delayed phenotypes are caused by Ku80-dependent mis-rejoining of delayed DNA double strand breaks. Mis-rejoining of DNA breaks and delayed induction of DNA double strand breaks were examined by chromosome analysis and 53BP1 foci analysis, respectively. As shown in Fig. 3, delayed induction of DNA double strand breaks was measured by 53BP1 foci in cells at 30–35 PDL post-irradiation. While the frequency of 53BP1 foci in the control CHO cells was approximately 0.14 ± 0.07, it was increased to 0.41 ± 0.19 in surviving cells. The frequency of 53BP1 foci in the unirradiated xrs5 cells was relatively higher (0.18 ± 0.08) compared to the CHO cells, and it was about 0.51 ± 0.27 in the surviving cells. Thus, it is indicated that delayed DNA damage was induced similarly in both CHO and xrs5 cells. Delayed chro-

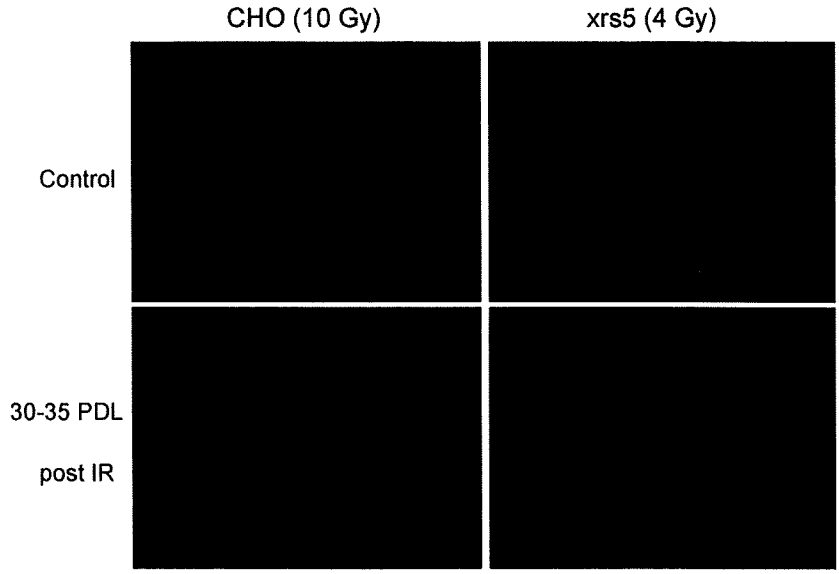

Fig. 3. Delayed DNA damage induction in cells 30–35 PDL after irradiation. Delayed induction of DNA double strand breaks was examined by 53BP1 foci formation. Both control and X-irradiated cells were fixed and stained with anti-53BP1 antibody as described in Section 2.

mosomal instability was examined at 15–20 PDL post-irradiation (Table 3) and 30–35 PDL post-irradiation (Table 4). We found that induction of chromatid breaks in xrs5 and xrs6 cells was comparable to CHO and EM9 cells. Interestingly, delayed formation of dicentric chromosomes was defective in xrs5 and xrs6 cells, while the control levels of dicentric chromosome were comparable among those cells. To confirm whether defective induction of dicentric chromosomes is related to Ku80-deficiency, delayed chromosomal instability was examined in the complimented xrs5 cells. We observed that delayed induction of dicentric chromosomes was increased to the level observed in CHO cells. Similar results were obtained in both cells at 15–20 PDL and 30–35 PDL post-irradiation. Delayed chromosomal instability was also examined in cells derived from DNA-PKcs-defective *Scid* mouse and ATM-knockout mouse (Table 5). Cells were irradiated with equivalent

Table 3
Delayed chromosomal instability in surviving cells at 15–20 PDL post-irradiation.

Cells	No. of cells with aberrations (%)			No. cells counted
	Dicentrics	Chromatid gaps/breaks	Others[a]	
CHO				
0 Gy	3(0.4)	24(3.0)	1(0.1)	801
8 Gy	37(4.4)	64(7.6)	5(0.6)	841
10 Gy	38(4.6)	93(11.2)	10(1.2)	832
EM9				
0 Gy	9(1.1)	30(3.6)	2(0.2)	841
6 Gy	30(3.5)	62(7.3)	15(1.8)	850
8 Gy	35(4.1)	82(9.6)	17(2.0)	857
xrs5				
0 Gy	8(1.0)	65(8.1)	2(0.3)	800
2 Gy	9(1.1)	119(14.8)	11(1.4)	805
4 Gy	13(1.6)	133(16.5)	8(1.0)	808
xrs6				
0 Gy	11(1.4)	64(8.0)	5(0.6)	802
2 Gy	16(2.0)	101(12.6)	12(1.5)	801
4 Gy	17(2.1)	98(12.0)	14(1.7)	818
xrs5/Ku80				
0 Gy	7(0.8)	26(3.1)	4(0.5)	827
8 Gy	28(3.1)	74(8.3)	8(0.9)	891
10 Gy	31(3.5)	85(9.7)	9(1.0)	876

[a] Rings, fragments and chromatid exchanges.

Table 4
Delayed chromosomal instability in surviving cells at 30–35 PDL post-irradiation.

Cells	No. of cells with aberrations (%)			No. cells counted
	Dicentrics	Chromatid gaps/breaks	Others[a]	
CHO				
0 Gy	4(0.5)	20(2.4)	0	828
8 Gy	44(5.3)	60(7.2)	4(0.5)	832
10 Gy	39(4.6)	112(13.2)	12(1.4)	848
EM9				
0 Gy	9(1.1)	31(3.7)	6(0.7)	840
6 Gy	52(6.1)	88(10.3)	12(1.4)	856
8 Gy	49(5.7)	124(14.5)	24(2.8)	858
xrs5				
0 Gy	8(1.0)	66(7.0)	8(1.0)	800
2 Gy	4(0.5)	92(11.3)	8(1.0)	816
4 Gy	12(1.3)	96(10.4)	8(0.9)	920
xrs6				
0 Gy	12(1.5)	56(6.9)	4(0.5)	812
2 Gy	16(1.7)	132(14.3)	8(0.9)	921
4 Gy	16(1.9)	116(14.1)	4(0.5)	824
xrs5/Ku80				
0 Gy	6(0.7)	26(3.1)	3(0.4)	849
8 Gy	32(3.7)	71(8.2)	5(0.6)	868
10 Gy	41(4.6)	96(10.7)	7(0.8)	897

[a] Rings, fragments and chromatid exchanges.

Table 5
Delayed chromosomal instability in surviving cells at 30–35 PDL post-irradiation.

Cells	No. of cells with dicentrics (%)	No. cells counted
CB17/wt		
0 Gy	8(2.2)	352
6 Gy	45(14.4)	313
CB17/SCID		
0 Gy	21(6.3)	331
2 Gy	62(17.4)	356
C3H/He ATM$^{+/+}$		
0 Gy	6(1.6)	376
6 Gy	59(15.4)	382
C3H/He ATM$^{-/-}$		
0 Gy	54(15.7)	345
3 Gy	115(32.0)	359

10% survival doses and delayed induction of dicentric chromosomes was analyzed 30–35 PDL post-irradiation. As shown in Table 5, the frequency of dicentric chromosomes in the unirradiated *Scid* and ATM-knockout cells was slightly higher than that in the wild-type cells, and increased dicentric frequencies in surviving cells were observed in both cases.

4. Discussion

It is well established that ionizing radiation induces delayed destabilization of the genome in the progeny of cells surviving ionizing radiation. Previously, several studies have demonstrated that delayed DNA double strand breaks are induced several generations after the initial insult [25,30,31], which has been proven by examining the delayed induction of foci of DNA damage checkpoint factors, such as phosphorylated histone H2AX. While phosphorylated histone H2AX foci are frequently used as biochemical markers for DNA double strand breaks, the foci of other DNA damage checkpoint factors, such as phosphorylated ATM foci and 53BP1 foci, are colocalized with phosphorylated histone H2AX foci [32–37], and they could also be used as alternative markers for DNA damage [38]. In the present study, we confirmed that the frequency of 53BP1 foci was higher in the progenies of surviving cells compared to unirradiated cells. Thus, it is quite reasonable to think that delayed induction of DNA double strand breaks in the progeny of surviving cells associated with pleiotropic manifestation of radiation-induced genomic instability.

Radiation-induced genomic instability has been reported commonly in various cell systems including human and rodent cells [11–14]. However, Chang and Little demonstrated that delayed reproductive death, one characteristic manifestation of radiation-induced genomic instability, was not observed in Ku80-deficient xrs5 cells [27]. The authors suggested that the cellular processing of DNA double strand breaks during repair must play a role in delayed reproductive death. Here, we found that not only delayed cell death but also delayed induction of giant cells and chromosome bridge were absent in xrs5 cells. Furthermore, other Ku80-deficient cell line, xrs6 [39], also revealed deficiency in the induction of those delayed phenotypes, while EM9 cells, defective in single-strand break repair, showed no apparent defect in delayed genomic instability induction. Thus, it was confirmed that DNA double strand break repair process is involved in the manifestation of delayed phenotypes. One possible explanation of the defective induction of some delayed phenotypes was that error-free DNA repair, such as homologous recombination, reduced the incidence of transmissible damage in the absence of error-prone NHEJ repair. If so, delayed induction of DNA double strand breaks was lower in Ku80-defective cells than the control CHO cells. Therefore, we checked whether delayed DNA damage was less frequent in xrs5 cells. The results clearly indicated that it was not the case, as we detected normal level of delayed induction of DNA damage in xrs5 cells. We also found that delayed chromatid breaks were similarly induced between Ku80-deficient cells and the wild-type cells (Tables 3 and 4). Thus, even without Ku80-dependent repair, genomic instability by itself could be induced in the progenies of surviving cells. Then, the second possibility was that defective NHEJ in xrs5 cells decreased the chance of mis-rejoining of the broken ends that occurred many generations after the initial insult. In fact, delayed induction of chromosome bridges between two daughter cells was significantly reduce in xrs5 and xrs6 cells (Table 2). Furthermore, delayed induction of dicentric chromosomes was completely absent in both xrs5 and xrs6 cells (Tables 3 and 4). Although several studies have reported that chromosome breakages are more frequent in ku80-deficient cells [40,41], the frequency of dicentric chromosome was relatively low considering the frequency of chromosome breaks [40]. These results supported our conclusion that the formation of dicentric chromosome caused by delayed DNA damage was compromised in Ku80-deficient cells. Although a back-up NHEJ may undertake mis-rejoining of broken ends in the absence of Ku-dependent NHEJ [42], it is highly likely that a major pathway of illegitimate rejoining the DNA breaks is Ku80-dependent process [43,44]. We also confirmed that radiation-induced genomic instability was manifested in cells derived from DNA-PKcs-defective *Scid* mouse. Moreover, delayed dicentric formation was normally detected in *Scid* cells. Therefore, DNA-PK-independent rejoining, which was suggested previously [45], is involved in delayed dicentric formation. Recently, it has been postulated that XRCC4/DNA Ligase IV-dependent but DNA-PKcs-independent rejoining needs Ku80/70 complex [5]. Thus, it is highly possible that Ku80-dependent mis-rejoining is involved in delayed generation of dicentric chromosomes, by which chromosome bridges are generated. Such mis-rejoining inhibits segregation of two daughter cells, which results in delayed induction of giant cells as well as delayed reproductive death.

It should be mentioned that delayed induction of chromatid breaks, observed in both surviving CHO and NHEJ-defective cells, could be a source of initiating ATM-dependent DNA damage checkpoint, which results in the execution of delayed cell death. However, defective p53 function in Chinese hamster cells incapacitates induction of irreversible cells cycle arrest and apoptosis in damaged cells [46,47]. Thus, although DNA breaks are associated with cells death in normal cells with the wild-type p53 function, it could not be a major cause of delayed cell death in Chinese hamster cells. Furthermore, it is well known that the broken ends are protected by telomere healing in rodent cells [48,49], which enables DNA damage checkpoint activation. Thus, although delayed chromatid breaks were induced in Ku80-deficient cells, they might not be involved in delayed reproductive death in Chinese hamster cells.

It should be very interesting to know the consequence of cells harboring such chromatid breaks. Previously, it was reported that ionizing radiation-induced genomic instability in the progeny of surviving CHO cells, which resulted in a heritable mutator phenotypes. For example, mutation frequency at the HPRT locus in surviving clones was persistently higher than the unirradiated progenies [50]. It was expected that such chromatid breaks caused large deletions at the HPRT locus, however, multiplex PCR analysis revealed that point mutations are the predominant type of genetic alterations in the mutants (data not shown). Because cells with micronuclei were frequently observed among the surviving cells, persistent chromatid breaks, which are not involved in delayed cell death under the p53-dysfunctional condition, may result in a loss of genetic materials. It has been proved that ionizing radiation induces delayed genomic instability, which accumulates genetic alterations including gene mutations, loss of heterozygosity, and chromosome rearrangements, concurrently with delayed reproductive death [11–14]. As Ku80-deficiency compromised delayed cell death through the formation of dicentric chromosomes, it is likely that cells with defective DNA repair capacity are more susceptible to carcinogenesis induced by DNA damaging agents [51].

Our present study demonstrated that DNA repair pathway is an important determinant of cellular response to ionizing radiation not only in the immediate response but also in cells surviving radiation exposure. Survived cells induced DNA double strand breaks many generations after the initial insult. Although the mechanism of delayed DNA damage induction has to be determined, delayed dicentric formation indicated that delayed DNA damage was induced in G1 phase. Such delayed DNA damage could be repaired by NHEJ repair, but it also provided a chance to engender mis-rejoining. These results should bring a new insight into how DNA repair protects the integrity of the genome from the insults of DNA damaging agents.

Conflict of interest

The authors declare that there are no conflicts of interest.

Acknowledgements

This work was supported in part by grants for scientific research and by the Global COE program from the Ministry of Education, Culture, Sports, Science, and Technology, Japan. The authors greatly appreciated Dr. Penny A. Jeggo for providing the plasmid containing the human Ku86 gene.

References

[1] E.C. Friedberg, DNA damage and repair, Nature 421 (2003) 436–440.
[2] D.M. Weinstock, C.A. Richardson, B. Elliott, M. Jasin, Modeling oncogenic translocations: distinct roles for double-strand break repair pathways in translocation formation in mammalian cells, DNA Repair 5 (2006) 1065–1074.
[3] C. Wynman, R. Kannar, DNA double strand break repair: all's well that ends well, Annu. Rev. Genet. 40 (2006) 363–383.
[4] P.A. Jeggo, M. Lobrich, DNA double-strand breaks: their cellular and clinical impact? Oncogene 26 (2007) 7717–7719.
[5] B.L. Mahaney, K. Meek, S.P. Lees-Miller, Repair of ionizing radiation-induced DNA double-strand breaks by non-homologous end-joining, Biochem. J. 417 (2009) 639–650.
[6] A. Pastink, J.C. Eeken, P.H. Lohman, Genomic integrity and the repair of double-strand breaks, Mutat. Res. 480/481 (2001) 37–50.
[7] D.C. van Gent, J.H. Hoeijmakers, R. Kannar, Chromosomal stability and the DNA double-stranded break connection, Nat. Rev. Genet. 2 (2001) 196–206.
[8] S. Burma, B.P. Chen, D.J. Chen, Role of non-homologous end joining (NHEJ) in maintaining genomic integrity, DNA Repair 5 (2006) 1042–1048.
[9] E. Sonoda, H. Hochegger, A. Saberi, Y. Taniguchi, S. Takeda, Differential usage of non-homologous end-joining and homologous recombination in double strand break repair, DNA Repair 5 (2006) 1021–2129.
[10] E.A. Leonhardt, M. Trinh, K. Chu, W.C. Dewey, Evidence that most radiation-induced HPRT mutants are generated directly by the initial radiation exposure, Mutat. Res. 426 (1999) 23–30.
[11] W.F. Morgan, J.P. Day, M.I. Kaplan, E.M. McGhee, C.L. Limoli, Genomic instability induced by ionizing radiation, Radiat. Res. 146 (1996) 247–258.
[12] J.B. Little, Genomic instability and bystander effects: a historical perspective, Oncogene 22 (2003) 6978–6987.
[13] S.A. Lorimore, P.J. Coates, E.G. Wright, Radiation-induced genomic instability and bystander effects: inter-related nontargeted effects of exposure to ionizing radiation, Oncogene 22 (2003) 7058–7069.
[14] K. Suzuki, M. Ojima, S. Kodama, M. Watanabe, Radiation-induced DNA damage and delayed induced genomic instability, Oncogene 22 (2003) 6988–6993.
[15] M.A. Kadhim, D.A. MacDonald, D.T. Goodhead, S.A. Lorimore, S.J. Marsden, E.G. Wright, Transmission of chromosomal instability after plutonium alpha-particle irradiation, Nature 355 (1992) 738–740.
[16] K. Suzuki, Multistep nature of X-ray-induced neoplastic transformation in mammalian cells: genetic alteration and instability, J. Radiat. Res. 38 (1997) 55–63.
[17] L. Huang, A.R. Snyder, W.F. Morgan, Radiation-induced genomic instability and its implications for radiation carcinogenesis, Oncogene 22 (2003) 5848–5854.
[18] O. Niwa, Induced genomic instability in irradiated germ cells and in the offspring; reconciling discrepancies among the human and animal studies, Oncogene 22 (2003) 7078–7086.
[19] E.I. Azzam, S.M. de Toledo, J.B. Little, Oxidative metabolism, gap junctions and the ionizing radiation-induced bystander effect, Oncogene 22 (2003) 7050–7057.
[20] C.L Limoli, E. Giedzinski, W.F. Morgan, S.G. Swarts, G.D. Jones, W. Hyun, Persistent oxidative stress in chromosomally unstable clones, Cancer Res. 63 (2003) 3107–3111.
[21] G.J. Kim, G.M. Fiskum, W.F. Morgan, A role for mitochondrial dysfunction in perpetuating radiation-induced genomic instability, Cancer Res. 66 (2006) 10377–10383.
[22] E.G. Wright, Microenvironment and genetic factors in haemopoietic radiation responses, Int. J. Radiat. Biol. 83 (2007) 813–818.
[23] P.J. Coates, J.K. Rundle, S.A. Lorimore, E.G. Wright, Indirect macrophage responses to ionizing radiation: implications for genotype-dependent bystander signaling, Cancer Res. 68 (2008) 450–456.
[24] J.H. Miller, S. Jin, W.F. Morgan, A. Yang, Y. Wan, U. Aypar, J.S. Peters, D.L. Springer, Profiling mitochondrial proteins in radiation-induced genome-unstable cell lines with persistent oxidative stress by mass spectrometry, Radiat. Res. 169 (2008) 700–706.
[25] K. Suzuki, S. Yokoyama, S. Waseda, S. Kodama, M. Watanabe, Delayed reactivation of p53 in the progeny of cells surviving ionizing radiation, Cancer Res. 63 (2003) 936–941.
[26] H. Toyokuni, A. Maruo, K. Suzuki, M. Watanabe, The contribution of radiation-induced large deletion of the genome to chromosomal instability, Radiat. Res. 171 (2009) 198–203.
[27] W.P. Chang, J.B. Little, Evidence that DNA double-strand breaks initiate the phenotype of delayed reproductive death in Chinese hamster ovary cells, Radiat. Res. 131 (1992) 53–59.
[28] A. Urushibara, S. Kodama, K. Suzuki, M.B.Md. Desa, F. Suzuki, T. Tsutsui, M. Watanabe, Involvement of telomere dysfunction in the induction of genomic instability by radiation in *scid* mouse cells, Biochem. Biophys. Res. Commun. 313 (2004) 1037–1043.
[29] B. Undarmaa, S. Kodama, K. Suzuki, O. Niwa, M. Watanabe, X-ray-induced telomeric instability in Atm-deficient mouse cells, Biochem. Biophys. Res. Commun. 315 (2004) 51–58.
[30] R.C. Barber, P. Hickenbotham, T. Hatch, D. Kelly, N. Topchiy, G.M. Almeida, G.D. Jones, G.E. Johnson, J.M. Parry, K. Rothkamm, Y.E. Dubrova, Radiation-induced transgenerational alterations in genome stability and DNA damage, Oncogene 25 (2006) 7336–7342.
[31] L. Huang, P.M. Kim, J.A. Nickoloff, W.F. Morgan, Targeted and nontargeted effects of low-dose ionizing radiation on delayed genomic instability in human cells, Cancer Res. 67 (2007) 1099–1104.
[32] J. Rouse, S.P. Jackson, Interfaces between the detection, signaling, and repair of DNA damage, Science 297 (2002) 547–551.
[33] M.B. Kastan, J. Bartek, Cell-cycle checkpoints and cancer, Nature 432 (2004) 316–323.
[34] J. Lukas, C. Lukas, J. Bartek, Mammalian cell cycle checkpoint-signalling pathways and their organization in space and time, DNA Repair 3 (2004) 997–1007.
[35] J.A. Downs, M.C. Nussenzweig, A. Nussenzweig, Chromatin dynamics and the preservation of genetic information, Nature 447 (2007) 951–958.
[36] J.W. Harper, S.J. Elledge, The DNA damage response: ten years after, Mol. Cell 28 (2007) 739–745.
[37] M.F. Lavin, S. Kozlov, ATM activation and DNA damage response, Cell Cycle 6 (2007) 931–942.
[38] M. Nakashima, K. Suzuki, S. Meirmanov, Y. Naruke, M. Matsuu-Matsuyama, K. Shichijo, V. Saenko, H. Kondo, T. Hayashi, M. Ito, S. Yamashita, I. Sekine, Foci formation of p53-binding protein 1 in thyroid tumors: activation of genomic instability during thyroid carcinogenesis, Int. J. Cancer 122 (2008) 1082–1088.
[39] B.K. Singleton, A. Priestley, H. Steingrimsdottir, D. Gell, T. Blunt, S.P. Jackson, A.R. Lehmann, P.A. Jeggo, Molecular and biochemical characterization of xrs mutants defective in Ku80, Mol. Cell. Biol. 17 (1997) 1264–1273.
[40] L.M. Kemp, P.A. Jeggo, Radiation-induced chromosome damage in X-ray-sensitive mutants (xrs) of the Chinese hamster ovary cell line, Mutat. Res. 166 (1986) 255–263.
[41] F. Darroudi, A.T. Natarajan, Cytogenetical characterization of Chinese hamster ovary X-ray-sensitive mutant cells xrs 5 and xrs 6. I. Induction of chromosomal aberrations by X-irradiation and its modulation with 3-aminobenzamide and caffein, Mutat. Res. 177 (1987) 133–148.
[42] G. Iliakis, H. Wang, A.R. Perrault, W. Boecker, B. Rosidi, F. Windhofer, W. Wu, J. Guan, G. Terzoudi, G. Pantelias, Mechanisms of DNA double strand break repair and chromosome aberration formation, Cytogenet. Genome Res. 104 (2004) 14–20.
[43] F. Liang, P.J. Romanienko, D.T. Weaver, P.A. Jeggo, M. Jasin, Chromosomal double-strand break repair in ku80-deficient cells, Proc. Natl. Acad. Sci. U.S.A. 93 (1996) 8929–8933.
[44] A.T. Natarajan, F. Palitti, DNA repair and chromosomal alterations, Mutat. Res. 657 (2008) 3–7.
[45] Y. Gao, J. Chaudhuri, C. Zhu, L. Davidson, D.T. Weaver, F.W. Alt, A targeted DNA-PKcs-null mutation reveals DNA-PK-independent functions for KU in V(D)J recombination, Immunity 9 (1998) 367–376.
[46] T. Hu, C.M. Miller, G.M. Ridder, M.J. Aardema, Characterization of p53 in Chinese hamster cell lines CHO-K1, CHO-WBL, and CHL: implications foe genotoxicity testing, Mutat. Res. 426 (1999) 51–62.
[47] B.S. Tzang, Y.C. Lai, M. Hsu, H.W. Chang, C.C. Chang, P.C. Huang, Y.C. Liu, Function and sequence analysis of tumor suppressor gene p53 of CHO.K1 cells, DNA Cell Biol. 18 (1999) 315–321.
[48] M.P. Hande, P.M. Lansdorp, A.T. Natarajan, Induction of telomerase activity by in vivo X-irradiation of mouse splenocytes and its possible role in chromosome healing, Mutat. Res. 404 (1998) 205–214.
[49] P. Slijepcevic, P.E. Bryant, Chromosome healing, telomere capture, and mechanisms of radiation-induced chromosome breakage, Int. J. Radiat. Biol. 73 (1998) 1–13.
[50] W.P. Chang, J.B. Little, Persistent elevated frequency of spontaneous mutations in progeny of CHO clones surviving X-irradiation: association with delayed reproductive death phenotypes, Mutat. Res. 270 (1992) 191–199.
[51] D.S. Lim, H. Vogel, D.M. Willefrod, A.T. Sands, K.A. Platt, P. Hasty, Analysis of ku80-mutant mice and cells with deficient levels of p53, Mol. Cell. Biol. 20 (2000) 3772–3780.

J. Radiat. Res., 50, 253–259 (2009)

Regular Paper

Introduction of a Normal Human Chromosome 8 Corrects Abnormal Phenotypes of Werner Syndrome Cells Immortalized by Expressing an h*TERT* Gene

Kentaro ARIYOSHI[1,7], Keiji SUZUKI[2], Makoto GOTO[3], Mitsuo OSHIMURA[4], Kanji ISHIZAKI[5], Masami WATANABE[6] and Seiji KODAMA[1]*

Werner syndrome/Chromosome transfer/Functional complementation.

Werner syndrome (WS) is an autosomal recessive disease characterized by premature aging and caused by mutations of the *WRN* gene mapped at 8p12. To examine functional complementation of WS phenotypes, we introduced a normal human chromosome 8 into a strain of WS fibroblasts (WS3RGB) immortalized by expressing a human telomerase reverse transcriptase subunit (h*TERT*) gene. Here, we demonstrate that the abnormal WS phenotypes including cellular sensitivities to 4-nitroquinoline-1-oxide (4NQO) and hydroxy urea (HU), and chromosomal radiosensitivity at G_2 phase are corrected by expression of the *WRN* gene mediated by introducing a chromosome 8. This indicates that those multiple abnormal WS phenotypes are derived from a primary, but not secondary, defect in the *WRN* gene.

INTRODUCTION

Werner syndrome (WS) is a rare autosomal recessive disorder characterized by the premature onset of a number of processes associated with aging.[1,2] The *WRN* gene, defected in WS, is mapped at 8p12 and encodes a WRN protein that is consisted of 1432-amino acids.[3] The WRN protein has both 3'→5' helicase and 3'→5' exonuclease activities[4,5] and has been suggested to function in DNA replication, repair and telomere processing.[6] The precise physiological roles of the WRN protein, however, remain to be obscure. Cells derived from WS patients show the hypersensitivities to selected DNA-damaging agents including 4-nitroquinoline-1-oxide (4NQO),[7,8] topoisomerase inhibitors,[9,10] DNA cross-linking agents[11] and hydroxy urea (HU).[12] In addition, WS cells demonstrate an abnormal radiation response at G_2 phase.[13] These studies suggest that the WRN protein plays an important role in DNA metabolism including DNA repair and replication pathways.

Because WS is caused by a defect of the *WRN* gene, it is highly expected that all abnormal phenotypes observed in WS cells can be rescued by expression of the *WRN* gene. To examine this anticipation, we introduced a normal human chromosome 8 into a SV 40-immortalized WS cell line by microcell fusion and studied functional complementation of the *WRN* gene.[14] However, we failed to complement abnormal phenotypes of the WS cells such as 4NQO hypersensitivity and a high incidence of spontaneous deletion mutation[15,16] in spite of expression of the WRN protein. This result raises the question whether the cellular abnormal phenotypes observed in WS cells are due to a primary effect or a secondary effect. On the other hand, it is also possible that secondary genetic changes due to the intrinsic instability of recipient SV40-immortalized WS cells might hamper a correction of abnormal phenotypes.

In the present study, to make clear these uncertainties concerning the complementation of the WS phenotype by the expression of the *WRN* gene, we introduced a normal human chromosome 8 into a WS cell line immortalized by expressing a human telomere reverse transcriptase subunit (h*TERT*) gene, and studied sensitivities to 4NQO and HU,

*Corresponding author: Phone: +81-72-254-9855,
Fax: +81-72-254-9855,
E-mail: kodama@riast.osakafu-u.ac.jp

[1]Radiation Biology Laboratory, Radiation Research Center, Frontier Science Innovation Center, Organization for University-Industry-Government Cooperation, Osaka Prefecture University, Sakai, Osaka 599-8570, Japan; [2]Course of Life Sciences and Radiation Research, Graduate School of Biomedical Sciences, Nagasaki University, Nagasaki 852-8523, Japan; [3]Division of Anti-Ageing and Longevity Sciences, Faculty of Biomedical Engineering, Toin University of Yokohama, Yokohama 225-8502, Japan; [4]Division of Molecular Genetics and Biofunction, Department of Biomedical Science, Institute of Regenerative Medicine and Biofunction, Graduate School of Medical Sciences, Tottori University, Yonago 683-8503, Japan; [5]Central Laboratory and Radiation Biology, Research Institute, Aich Cancer Center, Nagoya 464-8681, Japan; [6]Laboratory of Radiation Biology, Research Reactor Institute, Kyoto University, Osaka 590-0494, Japan; [7]Experimental Radiobiology for Children's Health Research Group, Research Center for Radiation Protection, National Institute of Radiological Sciences, Chiba 263-8555, Japan.
doi:10.1269/jrr.08111

and chromosome aberrations by X-irradiation at G_2 phase in microcell hybrids introduced with a human chromosome 8. In contrast to the previous study,[14] the expression of the *WRN* gene corrected the abnormal phenotypes examined.

MATERIALS AND METHODS

Cells and cell culture

Mouse A9 cells containing a single copy of human chromosome 8, which was tagged with a blasticidin S resistance gene, were used as chromosome donors. WS3RGB/T cells derived from WS3RGB fibroblasts (42-year-old female WS patient) were immortalized by introducing the h*TERT* gene and used as recipients. Normal human fibroblast cells immortalized by the h*TERT* gene, BJ/hTERT, were used as a control. The A9 cells were cultured in Dulbecco's modified Eagle's minimum essential medium (DMEM; Nissui Pharmaceutical, Tokyo) supplemented with 10% fetal bovine serum (FBS; Trace Bioscience, Melbourne), 100 U/ml penicillin, and 100 μg/ml streptomycin. WS3RGB/T cells and BJ/hTERT cells were cultured in α-modified minimum essential medium (α–MEM; Invitrogen, Carlsbad, CA) supplemented with 10% FBS, 100 U/ml penicillin, and 100 μg/ml streptomycin. Microcell hybrid (WS3RGB/T-8) cells were cultured in the α–MEM supplemented with 1.5 μg/ml blasticidin S (Funakoshi Co., Tokyo). Cells were maintained at 37°C in a humidified atmosphere with 5% CO_2.

Microcell Fusion

Microcell fusion was performed by the procedure described previously.[14] Briefly, donor cells (~1×10^6) were inoculated in 25-cm^2 flasks, and micronuclei were induced by treatment with 50 ng/ml Colcemid in the DMEM containing 20% FBS and 3 μg/ml blasticidin S for 48 h. The flasks were filled with serum free medium (SFM) containing 10 μg/ml cytochalasin B (Sigma Chemical Co., St. Louis, MO), and then micronuclei were isolated by centrifugation at 11,000 r.p.m. for 30 min at 34°C. The crude microcells were purified by filtration through a series of polycarbonate filters with pore sizes of 8, 5, and 3 μm. The purified microcells were resuspended in SFM containing 25 μg/ml phytohemagglutinin (Sigma Chemical Co., St. Louis, MO) and attached to the recipient WS3RGB/T cells by incubation at 37°C for 15 min. The cells were treated with 3 ml of polyethylene glycol (PEG; Sigma Chemical Co., St. Louis, MO) mixed with SFM (PEG : SFM, 1 : 1.4) for 30 sec, overlaid with 3 ml of a low-concentration PEG (PEG : SFM, 1 : 3) and treated for another 40 sec. After washing with SFM three times, the cells were filled with the α–MEM containing 10% FBS. After 48 h of incubation at 37°C, the recipient cells were replated for selection in the α–MEM containing 15% FBS and 1.5 μg/ml blasticidin S for 3–4 weeks. Blasticidin S-resistant microcell hybrids were isolated and grown in the α–MEM containing 10% FBS and 1.5 μg/ml blasticidin S.

Whole chromosome painting

Exponentially growing cells were treated with Colcemid (60 ng/ml) for 2 h and harvested. Chromosome samples were prepared as described previously.[14] For whole chromosome painting, the slide was air-dried overnight and immersed in pre-treatment solution (2X SSC / 0.5% NP-40, pH 7.0) for 30 min at 37°C. Then the slide was immersed in denaturing solution (70% formamide in 2X SSC, pH 7.0) for 3 min at 72°C. After dehydration by successive treatments with 70, 85 and 100% ethanol for each 2 min, the slide was dried with an airjet. A DNA probe that was specific for chromosome 8 (Q-Biogene, Montreal) was denatured at 72°C for 10 min and applied to a pre-warmed chromosome slide (45°C). The slide was covered with the probe mixture and glass coverslip and sealed with rubber cement to avoid evaporation. The hybridization was performed at 37°C for 16 h in the humidified atmosphere. After hybridization, the coverslip was removed, and the slide was incubated in wash buffer (0.5X SSC/ 0.1% SDS) for 5 min at 65°C, rinsed in PBD buffer (Q-Biogene, Montreal) at room temperature for 5 min, and stained with 8 μl of 20 ng/ml DAPI (Q-Biogene, Montreal) in antifade. The metaphase chromosomes were observed using a fluorescence microscope (Olympus, Tokyo) and digital images were recorded using a CCD camera (Olympus).

Expression of the WRN gene and protein

Expression of the *WRN* gene and protein in microcell hybrids was examined by reverse transcriptase-polymerase chain reaction (RT-PCR) and Western blotting, respectively, as described previously.[14,17] The relative expression of the *WRN* gene and protein was calculated from the band corresponding to the *WRN* gene and protein. The intensity of the band was adjusted by that corresponding to the *c-myc* gene for RT-PCR. For Western blotting analysis, the equal loading of protein was confirmed by Coomassie blue staining of the gels.

4NQO sensitivity

A 1 mM stock solution of 4NQO in ethanol (Wako Pure Chemical Industries, Osaka) was diluted with SFM prior to use. To examine cellular sensitivity to 4NQO, cells were plated into 100-mm dishes and cultured for 12 h. Then, the cells were washed once with SFM and treated with the SFM containing a graded concentration of 4NQO at 37°C for 1 h. After the treatment, the cells were washed once with complete culture medium, refed with the complete culture medium, and cultured for 14 days. Colonies more than 50 cells were scored as survivors.